



Statens vegvesen

Ferry free E39 – Fjord crossings Bjørnafjorden

304624

Rev.	Utgivelses dato	Beskrivelse	Laget av	Sjekk av	Prosj. godkj.	Klient godkj.
0	14.11.18	Issued for use	ES/HKF/ PJ/ØT	ØT		
Kunde	 Statens vegvesen					
Entreprenør	Kontrakt nr.:					

Dokument navn:

MetOcean Design basis

Dokument nr.:

SBJ-01-C4-SVV-01-BA-001

Rev.:

0

Sider:

53

Table of Contents

General

Nomenclature

Table of revisions

1	Wave data.....	3
1.1	Wind waves.....	3
1.2	Swell.....	4
1.3	Scatter diagram.....	5
1.3.1	Wind sea scatter diagram.....	5
1.3.2	Swell scatter diagram.....	7
1.4	Wave spectra.....	8
1.4.1	Wind sea.....	8
1.4.2	Swell.....	8
1.4.3	Directional spreading.....	8
1.5	Variation of wave conditions along bridge.....	9
1.6	Combination of wind, waves, swell and wind.....	11
1.6.1	Combination of wind and waves.....	11
1.6.2	Combination of wind seas and swell.....	12
1.7	Averaging period for waves.....	12
1.8	Waves from passing vessels.....	13
2	Wind.....	15
2.1	Return periods.....	15
2.1.1	Sectoral extremes.....	15
2.1.2	Distribution along the bridge.....	16
2.1.3	Wind profile.....	16
2.2	Turbulence intensity.....	16
2.3	Power spectral density of wind turbulence.....	17
3	Current.....	18
4	Water level variations.....	22
5	Water density variations.....	22
6	Temperature.....	23
6.1	Air temperature.....	23
6.2	Sea temperature.....	23
7	Climate change.....	23
8	References.....	25

Appendix A Wind Sea Scatter Diagrams and Contour plots

Appendix B Swell Scatter Diagrams

Appendix C Directional distribution of wind

Appendix D Distribution of Tidal Amplitudes

Appendix Ship Waves.xlsx

Appendix A.xlsx

Appendix B.xlsx

Appendix D.xlsx

General

This document gives the specifications for the meteorological and oceanographical data for the design of the bridge crossing of the Bjørnafjorden.

The parameters describing the metocean conditions are based on observations and reliable hindcast data from of the planned bridge crossing of Bjørnafjorden and areas nearby. The hindcast data has been validated with use of high quality physical measured data. To ensure proper length of the time series, synthetic data has been used to increase the quality of the hindcast data.

The references give the background for the design parameters given in this specification.

This work has been conducted according to the recommendations of N400 [1] chapter 5 and 13, the NORSE standard N-003, second edition “Actions and action effects” [2], and Det Norske Veritas (DNV) Recommended Practice DNV-RP-C205 “Environmental conditions and environmental loads” [3].

Nomenclature

H_s : significant wave height
 T_p : spectral peak period
 JONSWAP: JOint North Sea WAve Project
 σ_a & σ_b : JONSWAP spectral width parameters
 γ : JONSWAP non-dimensional peak shape parameter
 Γ : Gamma function
 V : wind speed
 z : height above sea level
 z_0 : roughness length
 k_T : terrain factor
 α : profile factor for the wind profile
 C_r : roughness factor
 k_{tt} : turbulence factor
 u, v, w : turbulence components
 I_u : longitudinal turbulence intensity
 I_v : lateral turbulence intensity
 I_w : vertical turbulence intensity
 n : frequency
 A_i : spectral density coefficients
 σ_i : standard deviation
 xL_i : turbulence length scale
 Δs_j : distance between points
 C_{ij} : coherence coefficients

1 Wave data

1.1 Wind waves

Design wave conditions for wind sea are based on simulations from [4], which is validated by measurements in [5].

Results are presented in terms of H_s/T_p contour lines for relevant return periods, contours for omni directional waves are presented in Figure 1, and remaining contour plots are given in Appendix E. For clarity, the peaks in the different contours are given in Table 1.

The different sectors refer to the direction from which the waves are coming from. $0^\circ/360^\circ$ means waves coming from the north, 90° coming from the east, 180° from the south and 270° from the west. Wave conditions are given as constant within each sector.

Return period / Sectors	1 year		10 year		50 year		100 year		10 000 year	
	H_s [m]	T_p [s]	H_s [m]	T_p [s]	H_s [m]	T_p [s]	H_s [m]	T_p [s]	H_s [m]	T_p [s]
Omni	1.3	4.3	1.7	4.8	2.0	5.2	2.1	5.3	2.9	6.1
345° - 15°	0.3	2.5	0.6	3.5	0.8	4.0	0.8	4.0	1.3	4.7
15° - 45°	0.2	1.9	0.5	3.3	0.7	4.2	0.7	4.2	1.2	4.9
45° - 75°	0.5	3.1	0.7	3.6	0.8	3.9	0.9	4.1	1.2	4.8
75° - 105°	1.0	4.0	1.5	4.7	1.9	5.2	2.1	5.5	3.1	6.5
105° - 135°	0.9	3.7	1.1	4.1	1.3	4.4	1.4	4.6	2.0	5.4
135° - 165°	0.9	3.4	1.1	3.8	1.2	4.0	1.2	4.0	1.6	4.7
165° - 195°	0.8	3.3	1.0	3.6	1.2	3.9	1.2	3.9	1.6	4.3
195° - 225°	0.9	3.7	1.2	4.3	1.3	4.4	1.4	4.6	1.8	5.2
225° - 255°	0.8	3.1	1.1	3.6	1.3	3.9	1.4	4.0	1.9	4.6
255° - 285°	1.0	3.5	1.4	4.0	1.7	4.4	1.8	4.5	2.7	5.3
285° - 315°	1.2	4.3	1.6	4.8	1.8	5.0	2.0	5.2	2.7	5.9
315° - 345°	0,7	3,7	0,9	4,1	1,1	4,5	1,2	4,6	1,7	5,3

Table 1: Wind generated waves, all year.

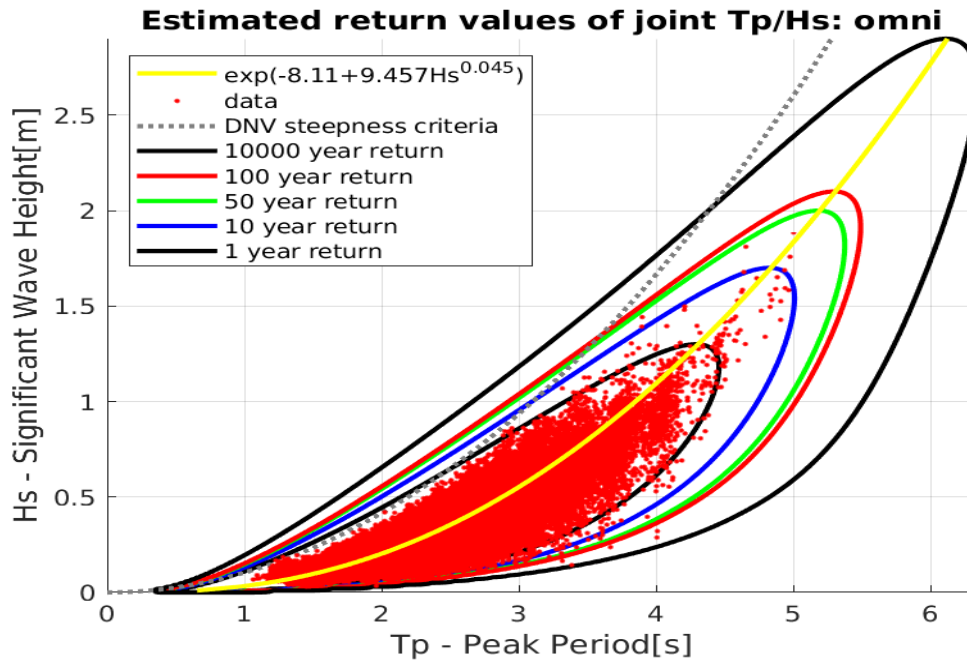


Figure 1: Contour plot for omni-directional sea waves.

1.2 Swell

The data for swell waves can be found from the Table 2 and Figure 2. Swell conditions in Bjørnafjorden are based on simulations performed by Norconsult [6].

Return period / Season	1 year Hs [m]	10 year Hs [m]	50 year Hs [m]	100 year Hs [m]	10 000 year Hs [m]
All year	0.22	0.28	0.33	0.34	0.46

Table 2: Significant wave height, swell.

The significant wave heights given in Table 2 are valid for peak periods from 12-20 seconds. Wave heights outside this period range can be found by correcting with the coefficients given in Figure 2. The basis for Figure 2 is described in [7].

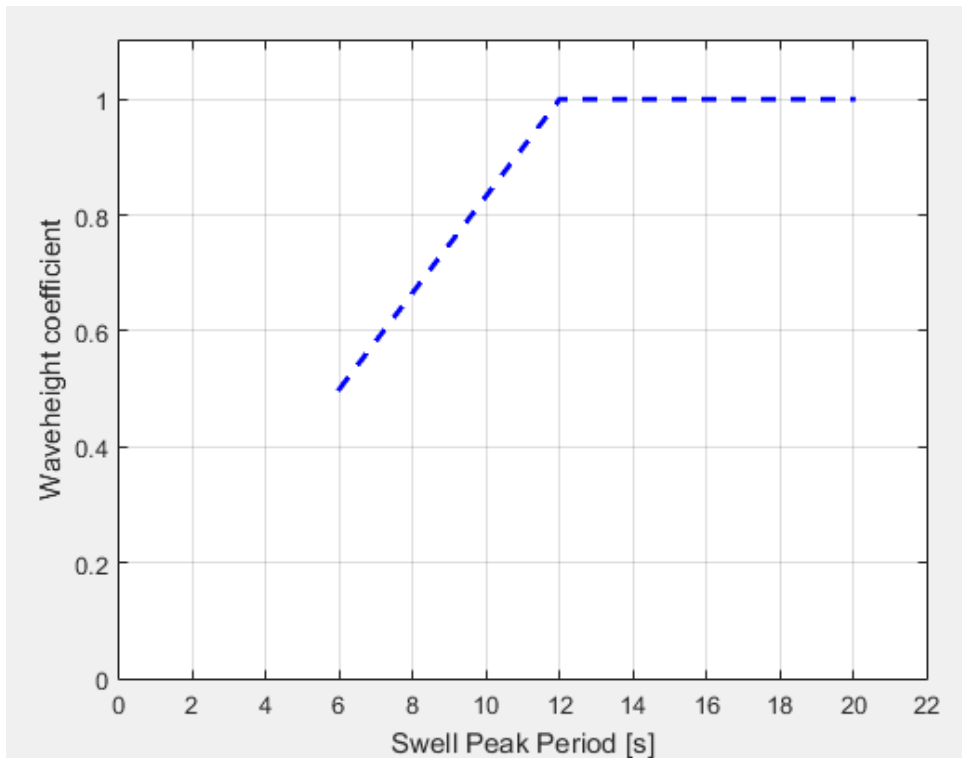


Figure 2: Swell peak periods.

Tabulated values of Figure 2 are given in Table 3.

Peak period [s]	6	7	8	9	10	11	12	18	20
$H_s/H_{s,max}$	0.50	0.58	0.67	0.75	0.83	0.92	1.0	1.0	1.0

Table 3: Swell peak periods.

The swell system consists of two contributions, one coming from the northwest (320°) and one coming from the south - southwest (205°). The contribution from northwest is dominating, and contains on average above 80% of the total wave energy from swell. Since the total wave energy from swell already is small, it is considered adequate to assume that all swell comes from north. Following this approach, the direction of swell shall be taken as the most unfavorable in the sector 300° - 330° .

1.3 Scatter diagram

Scatter diagrams for all year all directions are given in this report, see Table 4 and Table 5. Scatter diagrams for different sectors and months for wind sea and swell can be found in Appendix A and B respectively. All scatter diagrams are presented as percentage of occurrence.

The scatter diagrams are based on simulation/synthetic data of 15 years for wind sea and 37 years for swell. The scatter diagrams are to be used as input for fatigue analysis.

1.3.1 Wind sea scatter diagram

The wind sea scatter diagram is based on 15 years of simulated data. For more details on how the scatter diagram is established, the reader is referred to [4].

Wind Sea, Scatter diagram: All directions													
Hm0 [m]	Tp [s]											Sum	
	0.0 - 0.5	0.5 - 1.0	1.0 - 1.5	1.5 - 2.0	2.0 - 2.5	2.5 - 3.0	3.0 - 3.5	3.5 - 4.0	4.0 - 4.5	4.5 - 5.0	5.0 - 5.5		5.5 - 6.0
0.0 - 0.1			2,02E+01	2,30E+00	2,57E-01	7,44E-04							22,73
0.1 - 0.2			1,03E+01	1,49E+01	5,12E+00	6,14E-01	1,04E-02						30,95
0.2 - 0.3				5,24E+00	1,04E+01	2,37E+00	1,41E-01	2,98E-03	7,44E-04				18,12
0.3 - 0.4				1,34E-01	6,36E+00	4,79E+00	5,72E-01	1,04E-02	7,44E-04				11,87
0.4 - 0.5					1,22E+00	4,59E+00	1,31E+00	3,94E-02	0,00E+00				7,16
0.5 - 0.6					7,59E-02	1,90E+00	1,98E+00	1,27E-01	3,72E-03				4,08
0.6 - 0.7						5,39E-01	1,45E+00	3,23E-01	1,12E-02				2,32
0.7 - 0.8						8,04E-02	7,26E-01	5,02E-01	1,71E-02				1,33
0.8 - 0.9						8,93E-03	2,49E-01	4,51E-01	5,13E-02				0,76
0.9 - 1.0							5,95E-02	2,47E-01	6,92E-02				0,38
1.0 - 1.1								1,19E-02	5,80E-02	7,74E-02			0,15
1.1 - 1.2								7,44E-04	1,93E-02	4,47E-02	7,44E-04		0,07
1.2 - 1.3									3,72E-03	3,42E-02	2,23E-03		0,04
1.3 - 1.4									1,49E-03	1,49E-02	5,95E-03		0,02
1.4 - 1.5									7,44E-04	2,98E-03	6,70E-03		0,01
1.5 - 1.6											6,70E-03		0,01
1.6 - 1.7											2,98E-03		0,00
1.7 - 1.8											7,44E-04		0,00
1.8 - 1.9											7,44E-04	7,44E-04	0,00
1.9 - 2.0													0,00
Sum	0,00	0,00	30,46	22,61	23,39	14,90	6,50	1,79	0,33	0,03	0,00	0,00	100,00

Table 4: Wind sea, all year scatter diagram.

1.3.2 Swell scatter diagram

Note that the upper left bin in Table 6 ($0 < H_s < 0.01$ & $T_p < 2$), represents sea states where there are no swell present. The swell scatter is based on 37 years of synthetic data from [6]. Peak periods have been smoothed, more detail on this approach can be found in [7].

Hm0		Tp																			Sum				
		<2	2 - 3	3 - 4	4 - 5	5 - 6	6 - 7	7 - 8	8 - 9	9 - 10	10 - 11	11 - 12	12 - 13	13 - 14	14 - 15	15 - 16	16 - 17	17 - 18	18 - 19	19 - 20		>20			
0,00	0,01	60,9633				1,6344	1,4060	1,1692	1,4633	1,5049	1,4448	1,1229	0,6123	0,3330	0,1545	0,0990	0,0351	0,0139	0,0037						71,9603
0,01	0,02					0,5291	1,2987	0,9278	1,1238	1,1127	0,9925	0,8491	0,7825	0,5291	0,3043	0,1609	0,0647	0,0277	0,0111					0,0018	8,7160
0,02	0,03					0,0990	0,3894	0,7853	0,4357	0,6299	0,6993	0,6151	0,6586	0,4542	0,2969	0,1924	0,0509	0,0231	0,0148				0,0037	0,0018	5,3501
0,03	0,04					0,0028	0,0583	0,7233	0,5272	0,2118	0,3663	0,3950	0,3200	0,2756	0,2183	0,1304	0,0555	0,0203	0,0102				0,0009		3,3160
0,04	0,05						0,0018	0,4486	0,8834	0,3857	0,1045	0,1841	0,2229	0,1554	0,1572	0,1258	0,0620	0,0250	0,0139						2,7703
0,05	0,06							0,1720	0,7169	0,6225	0,1350	0,0684	0,1165	0,0601	0,0684	0,0601	0,0573	0,0176	0,0157				0,0009		2,1117
0,06	0,07								0,0564	0,4199	0,7261	0,2951	0,0610	0,0462	0,0314	0,0287	0,0296	0,0462	0,0222	0,0139					1,7769
0,07	0,08								0,0166	0,1323	0,4116	0,3330	0,0675	0,0166	0,0176	0,0157	0,0166	0,0157	0,0111	0,0120			0,0018		1,0683
0,08	0,09								0,0018	0,0268	0,2405	0,3959	0,1267	0,0157	0,0074	0,0046	0,0046	0,0046	0,0028	0,0120					0,8436
0,09	0,10									0,0046	0,1119	0,2830	0,1933	0,0166	0,0009	0,0028	0,0028	0,0028	0,0046	0,0037					0,6271
0,10	0,11										0,0361	0,1794	0,1545	0,0166	0,0037	0,0009		0,0009	0,0037	0,0018					0,3977
0,11	0,12											0,0102	0,1008	0,1526	0,0305	0,0018	0,0018		0,0009	0,0028					0,3034
0,12	0,13												0,0009	0,0074	0,0472	0,1073	0,0518	0,0092	0,0009	0,0018	0,0009				0,2266
0,13	0,14														0,0157	0,0444	0,0601	0,0111	0,0009	0,0009					0,1369
0,14	0,15															0,0028	0,0213	0,0657	0,0166	0,0028	0,0009				0,1128
0,15	0,16																0,0018	0,0250	0,0731	0,0176	0,0037	0,0009	0,0009	0,0009	0,1239
0,16	0,17																		0,0120	0,0370	0,0111	0,0055	0,0009		0,0666
0,17	0,18																		0,0055	0,0231	0,0102	0,0018	0,0028		0,0444
0,18	0,19																			0,0129	0,0046	0,0028	0,0018		0,0250
0,19	0,20																				0,0009	0,0009	0,0028	0,0046	0,0102
0,20	0,21																					0,0009	0,0018	0,0009	0,0102
0,21	0,22																								0,0009
0,22	0,23																								0,0009
Sum		60,9633	0,0000	0,0000	0,0000	2,2653	3,1542	4,3011	5,7348	6,0114	5,3972	4,2077	3,1828	1,9545	1,2829	0,8325	0,3968	0,1804	0,1239	0,0074	0,0037				100,0000

Table 5: Swell, all year scatter diagram.

1.4 Wave spectra

1.4.1 Wind sea

By comparing spectrums from both simulations and measurements, we see that the JONSWAP spectra fits reasonable well to the locally wind generated waves in the fjord. JONSWAP with average spectral width ($\sigma_a=0.07$ and $\sigma_b=0.09$) can be used, the gamma parameter shall be varied in the range $\gamma = 1.8 - 2.3$. The JONSWAP definition from DNV-RP-C205 [3] shall be used, this definition is given below.

$$S_j(\omega) = A_\gamma \cdot \frac{5}{16} \cdot H_s^2 \cdot \omega_p^4 \cdot \omega^{-5} \cdot \exp\left(-\frac{5}{4} \left(\frac{\omega}{\omega_p}\right)^{-4}\right) \cdot \gamma \cdot \exp\left(-0.5 \left(\frac{\omega - \omega_p}{\sigma \cdot \omega_p}\right)^2\right)$$

where

$$A_\gamma = 1 - 0.287 \cdot \ln(\gamma)$$

γ – non – dimensional peak shape parameter

ω – Radial frequency

$$\omega_p = \frac{2\pi}{T_p}$$

σ – spectral width parameter

$$\sigma = \sigma_a \text{ for } \omega \leq \omega_p$$

$$\sigma = \sigma_b \text{ for } \omega > \omega_p$$

1.4.2 Swell

Presently we do not have theoretical wave spectra that fits the simulated swell conditions very well. There could be an option to run with the numerical spectra from the wave simulations. Instead, it is decided that JONSWAP spectra should be used for swell, with a gamma value between 3 and 5.

With this simplification, the wave energy from swell is represented by a narrower and steeper wave spectrum than one can expect from the actual wave spectrum. It is therefore crucial that a detailed screening of the wave periods are performed, if not, there is a significant risk that the wave energy at important resonant frequencies will be underestimated.

1.4.3 Directional spreading

Directional spreading for wind sea is defined in Table 6.

The incoming swell has low directional spreading and shall be taken as given in Table 6 or as longcrested waves, whichever gives the largest response. Recommended values for directional spreading is given in Table 6. The formula for the cos n distribution below, is taken from DNV-RP-C205 [3].

Directional spreading / Wave system	n
Wind Sea	3-8
Swell	10-20

Table 6: Directional spreading parameters for a cos-n distribution.

$$D(\theta) = \frac{\Gamma\left(1 + \frac{n}{2}\right)}{\sqrt{\pi}\Gamma\left(\frac{1}{2} + \frac{n}{2}\right)} \cos^n(\theta - \theta_p)$$

Γ – Gamma function

θ_p – Main wave direction

θ – Angle between the direction of elementary wave trains and the main wave direction

1.5 Variation of wave conditions along bridge

In this section it is presented results which can be used to account for varying wind wave conditions along the bridge. Swell conditions should be considered as constant along the bridge.

In order to present the variation of wind wave conditions along the bridge crossing, results are extracted from the model results at a straight line between Svarvhelleholmen and Gullholmane, and is referred to results at the center of the crossing. The center of the crossing is the location of all extreme statistics and scatter diagrams.

The location and origin of the data points used to present these results are given in Figure 3.



Figure 3: Overview of the location of the data points.

How the wave conditions vary along the bridge will to a large degree depend on the incoming wave direction, therefore appropriate scaling factors are calculated for each wave sector. Scaling factors for significant wave height can be found in Table 7.

Correction factors for varying significant wave height along bridge												
Position along line, x [m] (x=0 south)	Sector											
	1	2	3	4	5	6	7	8	9	10	11	12
	345	15	45	75	105	135	165	195	225	255	285	315
	15	45	75	105	135	165	195	225	255	285	315	345
400	1.28	1.21	1.16	0.82	0.65	0.49	0.34	0.35	0.57	0.79	1.06	1.19
600	1.26	1.20	1.15	0.86	0.70	0.56	0.44	0.45	0.64	0.83	1.07	1.18
800	1.25	1.19	1.14	0.88	0.74	0.62	0.52	0.53	0.69	0.86	1.07	1.17
1000	1.23	1.17	1.13	0.91	0.78	0.68	0.60	0.61	0.74	0.89	1.07	1.16
1200	1.21	1.16	1.12	0.93	0.81	0.73	0.67	0.68	0.79	0.91	1.07	1.14
1400	1.18	1.14	1.11	0.95	0.85	0.77	0.73	0.74	0.83	0.93	1.06	1.12
1600	1.16	1.12	1.10	0.96	0.87	0.82	0.79	0.80	0.86	0.94	1.05	1.10
1800	1.13	1.10	1.08	0.98	0.90	0.86	0.84	0.84	0.89	0.96	1.04	1.09
2000	1.10	1.08	1.06	0.99	0.93	0.89	0.88	0.89	0.92	0.97	1.03	1.07
2200	1.07	1.06	1.04	0.99	0.95	0.93	0.92	0.93	0.95	0.98	1.02	1.05
2400	1.04	1.03	1.02	1.00	0.97	0.96	0.96	0.96	0.97	0.99	1.01	1.03
2600	1.00	1.00	1.00	1.00	1.00	1.00	0.99	1.00	1.00	1.00	1.00	1.00
2800	0.96	0.97	0.97	1.00	1.02	1.03	1.03	1.03	1.02	1.01	0.99	0.98
3000	0.92	0.93	0.94	1.00	1.04	1.05	1.06	1.05	1.04	1.01	0.97	0.95
3200	0.87	0.89	0.91	1.00	1.05	1.08	1.08	1.08	1.06	1.02	0.94	0.91
3400	0.82	0.84	0.87	0.99	1.07	1.11	1.11	1.10	1.08	1.02	0.91	0.86
3600	0.75	0.78	0.83	0.99	1.08	1.13	1.13	1.12	1.09	1.02	0.87	0.80
3800	0.68	0.72	0.79	0.98	1.10	1.16	1.15	1.14	1.10	1.01	0.81	0.73
4000	0.60	0.64	0.74	0.97	1.11	1.18	1.17	1.16	1.11	1.00	0.74	0.64
4200	0.51	0.56	0.69	0.96	1.11	1.19	1.18	1.17	1.12	0.98	0.65	0.53
4400	0.40	0.46	0.63	0.95	1.11	1.21	1.20	1.18	1.12	0.94	0.53	0.40
4800	0.40	0.46	0.63	0.95	1.11	1.21	1.20	1.18	1.12	0.94	0.53	0.40

Table 7: Scaling factors for significant wave height.

Varying spectral peak period is presented on a similar format in Table 8.

Correction factors for varying spectral peak period along bridge												
Position along line, x [m] (x=0 south)	Sector											
	1	2	3	4	5	6	7	8	9	10	11	12
	345	15	45	75	105	135	165	195	225	255	285	315
	15	45	75	105	135	165	195	225	255	285	315	345
400	1.01	1.04	1.04	0.99	1.00	0.80	0.51	0.48	0.84	0.97	1.03	1.05
600	1.00	1.05	1.04	1.00	1.00	0.82	0.55	0.56	0.85	0.97	1.03	1.04
800	0.99	1.06	1.04	1.00	1.00	0.83	0.60	0.64	0.87	0.98	1.02	1.03
1000	0.99	1.06	1.04	1.00	1.00	0.85	0.64	0.70	0.88	0.98	1.02	1.02
1200	0.98	1.07	1.04	1.00	1.00	0.87	0.69	0.76	0.90	0.98	1.02	1.02
1400	0.98	1.06	1.03	1.00	1.00	0.88	0.73	0.81	0.91	0.98	1.01	1.01
1600	0.98	1.06	1.03	1.00	1.00	0.90	0.78	0.86	0.92	0.98	1.01	1.01
1800	0.98	1.05	1.02	1.00	1.00	0.92	0.82	0.90	0.94	0.99	1.01	1.01
2000	0.98	1.04	1.02	1.00	1.00	0.94	0.86	0.93	0.95	0.99	1.01	1.01
2200	0.98	1.02	1.01	1.00	1.00	0.96	0.90	0.96	0.97	0.99	1.01	1.01
2400	0.98	1.01	1.01	1.00	1.00	0.98	0.94	0.98	0.98	1.00	1.01	1.01
2600	0.97	0.98	1.00	1.00	1.00	1.00	0.97	1.00	1.00	1.00	1.01	1.01
2800	0.96	0.96	0.99	1.00	1.00	1.01	1.00	1.02	1.01	1.00	1.00	1.01
3000	0.94	0.93	0.99	1.00	1.00	1.03	1.02	1.03	1.02	1.01	1.00	1.00
3200	0.92	0.89	0.98	1.00	1.01	1.04	1.04	1.04	1.03	1.01	0.99	1.00
3400	0.89	0.85	0.97	0.99	1.01	1.05	1.06	1.05	1.04	1.01	0.98	0.99
3600	0.85	0.81	0.96	0.99	1.01	1.06	1.06	1.05	1.05	1.01	0.96	0.98
3800	0.81	0.76	0.96	0.99	1.02	1.06	1.07	1.05	1.06	1.01	0.94	0.96
4000	0.76	0.70	0.95	0.99	1.02	1.07	1.06	1.05	1.07	1.01	0.92	0.94
4200	0.69	0.64	0.94	0.99	1.03	1.07	1.06	1.06	1.07	1.01	0.90	0.92
4400	0.62	0.58	0.93	0.99	1.03	1.07	1.04	1.06	1.07	1.01	0.87	0.89
4800	0.62	0.58	0.93	0.99	1.03	1.07	1.04	1.06	1.07	1.01	0.87	0.89

Table 8: Scaling factors for spectral peak period.

1.6 Combination of wind, waves, swell and wind

1.6.1 Combination of wind and waves

Wind waves and wind are generally well correlated. Consequently, extreme wind sea should be combined with wind conditions with the same return period.

Correlation of wind and waves to be used for fatigue analysis can be based on average wind velocities within each sector, given in Table 9. The table is established based on input wind velocity and direction used to establish the wind sea scatter diagrams. For more information see [7].

		Correlated 1 hour wind speed [m/s]											
Direction [°] /		0°	30°	60°	90°	120°	150°	180°	210°	240°	270°	300°	330°
Hs [m]		345° - 15°	15° - 45°	45° - 75°	75° - 105°	105° - 135°	135° - 165°	165° - 195°	195° - 225°	225° - 255°	255° - 285°	285° - 315°	315° - 345°
0.00 - 0.10		2.12	2.14	2.39	2.59	2.49	2.35	2.11	2.18	2.21	2.19	2.24	2.20
0.10 - 0.20		2.73	2.49	3.25	3.86	3.93	4.06	3.61	3.82	3.96	3.89	3.60	3.13
0.20 - 0.30		5.15	4.93	4.72	5.38	5.70	6.06	5.63	5.64	6.07	5.59	4.97	4.95
0.30 - 0.40		6.28	5.95	6.04	6.63	7.17	7.44	6.91	7.00	7.66	7.11	6.30	6.18
0.40 - 0.50		7.44	8.64	7.20	7.75	8.53	8.94	8.33	8.52	8.93	8.27	7.51	7.25
0.50 - 0.60		8.67	9.13	8.19	8.60	10.03	10.47	9.77	9.81	10.44	9.59	8.58	8.32
0.60 - 0.70		11.43		9.70	9.42	10.95	11.79	11.01	11.47	11.83	10.85	9.77	9.52
0.70 - 0.80		10.78			10.47	12.10	13.33	12.65	12.62	13.44	12.19	10.63	9.95
0.80 - 0.90		12.86			11.28	12.73	14.16	13.79	14.02	14.41	13.59	11.78	10.69
0.90 - 1.00					12.20	14.01	14.66	14.40	14.94	15.26	14.71	12.77	
1.00 - 1.10					13.68	14.27	16.43	14.73	16.08	17.22	16.33	13.90	
1.10 - 1.20					14.01	16.69	16.85		19.57	16.11	16.83	14.66	
1.20 - 1.30					15.95				20.06		20.18	15.56	
1.30 - 1.40					14.88				15.70		21.05	17.25	
1.40 - 1.50					15.94						17.48	18.64	
1.50 - 1.60					17.79							17.02	
1.60 - 1.70												19.88	
1.70 - 1.80												19.80	
1.80 - 1.90												23.28	

Table 9 Correlated wind speed.

The wind direction will not necessarily follow the wave direction. For severe environmental conditions the directions tend to be similar for the most part, whereas for smaller sea states there appear to be little or no connection. This is presented this in Table 10. For each sector with wave directions and Hs interval, the mean wind direction is calculated along with a 90% confidence band (+/- in the table). There are instances in this table for the larger wave heights where the confidence limits is small and even goes to zero. It seems quite clear that the trend is less spreading for more severe storm conditions, but a small population of data for these conditions also seems like a reasonable explanation. Therefore it is recommended that the confidence limits are never taken smaller than +/- 15 degrees.

Wind direction and 90% confidence intervals for given wave sectors																								
Hs [m]	Wind direction																							
	Sector 1 345 - 15		Sector 2 15 - 45		Sector 3 45 - 75		Sector 4 75 - 105		Sector 5 105 - 135		Sector 6 135 - 165		Sector 7 165 - 195		Sector 8 195 - 225		Sector 9 225 - 255		Sector 10 255 - 285		Sector 11 285 - 315		Sector 12 315 - 345	
	Mean	+/-	Mean	+/-	Mean	+/-	Mean	+/-	Mean	+/-	Mean	+/-	Mean	+/-	Mean	+/-	Mean	+/-	Mean	+/-	Mean	+/-	Mean	+/-
0.0 - 0.1	16	161	52	149	78	124	88	104	109	117	139	134	165	146	191	149	211	156	260	166	313	159	343	167
0.1 - 0.2	7	129	41	142	71	96	97	63	122	71	147	76	163	97	191	87	227	100	267	86	307	87	341	104
0.2 - 0.3	6	47	0	51	67	47	99	41	131	43	152	39	168	49	199	46	231	46	258	53	313	48	347	42
0.3 - 0.4	7	38	18	55	63	43	102	35	135	38	154	32	170	36	200	39	232	39	257	44	317	37	349	31
0.4 - 0.5	9	19	26	44	58	54	103	39	139	37	157	29	173	33	201	33	236	33	258	40	320	30	347	23
0.5 - 0.6	351	18	358	0	58	34	102	38	140	30	160	22	174	25	201	29	234	33	260	33	320	32	348	20
0.6 - 0.7	2	19			60	23	100	33	140	29	162	21	173	22	201	24	236	23	258	32	320	26	346	19
0.7 - 0.8	4	16					98	28	139	28	159	22	177	24	200	23	240	29	259	28	318	26	343	19
0.8 - 0.9	6	18					104	27	144	39	159	32	175	30	198	21	241	23	260	29	319	29	348	14
0.9 - 1.0							101	31	144	22	157	20	174	11	199	21	242	31	262	27	312	31		
1.0 - 1.1							103	23	150	17	151	7	178	0	201	22	245	22	260	29	308	28		
1.1 - 1.2							103	28	147	0	154	0			221	12	237	4	261	17	308	31		
1.2 - 1.3							104	19							197	0			254	19	315	26		
1.3 - 1.4							94	30							207	0			266	11	315	28		
1.4 - 1.5							99	7											302	28	308	17		
1.5 - 1.6							103	9													309	7		
1.6 - 1.7																					310	6		
1.7 - 1.8																					304	0		
1.8 - 1.9																					297	2		
1.9 - 2.0																								

Table 10 Wind direction and 90% confidence intervals for given wave sectors.

A table with the directional distribution of wind for each wave sector is found in Appendix C.

1.6.2 Combination of wind seas and swell

From [6] it is seen that even severe storms give low amount of wave energy from swell at the bridge crossing. The wind direction and thereby the wind wave direction for both offshore and inshore waves are fairly correlated for larger events. This means that large storms with wind coming from westerly directions are likely to give both large wind sea and swell at the bridge location. For that reason, wind sea from westerly directions (180° - 360°) shall be combined with swell.

Wind sea from easterly directions are not likely to see any significant contributions from swell, of course offshore swell could in principal give some swell seas at the bridge site, even for fairly severe easterly storms. The wave heights for offshore swell are small, and it is thought that the swell energy at the bridge crossing will be negligible for such events. Wind sea from easterly directions (0° - 180°) shall not be combined with swell.

1.7 Averaging period for waves

This document does not instruct the reader to whether analysis shall be run with 1-hour or 3-hour simulations. The significant wave heights presented herein are all given as 1-hour values, which can be used directly as input for 1-hour simulations.

Swell is originally calculated as 3-hour significant wave heights, which is corrected to 1-hour by a 9% increase. These can be corrected back to 3-hour with a correction factor of 0.917.

The significant wave height for wind seas are calculated as 1-hour values without any correction. The reduction factor to be used to convert the significant wave height to 3-hour values will be dependent on which return period is corrected. It is proposed that the correction is done in accordance with [8], which is given in Table 11.

Return period	Correction factor (1-hour to 3-hour Hs)
1	0.917
10	0.934
50	0.942
100	0.945
10 000	0.959

Table 11: Wind seas, correction factor from 1-hour Hs to 3-hour Hs

1.8 Waves from passing vessels

During the ongoing measurement campaign in Bjørnafjorden, there has been observed a significant number of cases that are presently believed to be waves induced by passing vessels. Many of these cases give waves with periods around 6 seconds. The periods of vessel generated waves are dependent on the vessel speed; 20 knots gives waves with periods around 6 seconds, which is a case that matches fairly well with the ferries crossing Bjørnafjorden.

When a bridge is built sometime in the future, there will most likely be traffic control of the ship traffic in the area, and in that context a speed limit around 12 knots have been suggested. With a speed limit of 12 knots, the wave periods of vessel generated waves will be so short that the wave energy of such events will be negligible compared to the wave energy from wind driven seas.

But even if speed restrictions are enforced in Bjørnafjorden when the bridge is completed, the concepts need to be robust enough to withstand the loading from waves generated by rogue vessels that do not follow these speed restrictions.

The following cases with vessel generated waves shall be considered for the concepts as ALS-cases, as shown in Figure 4. The time series are established with a time step of 0.1s, and are therefore considered impractical to include as tables in an Appendix. Time series will be made available to the project groups by an excel sheet. For more information on how these time series are established, the reader is referred to [7]

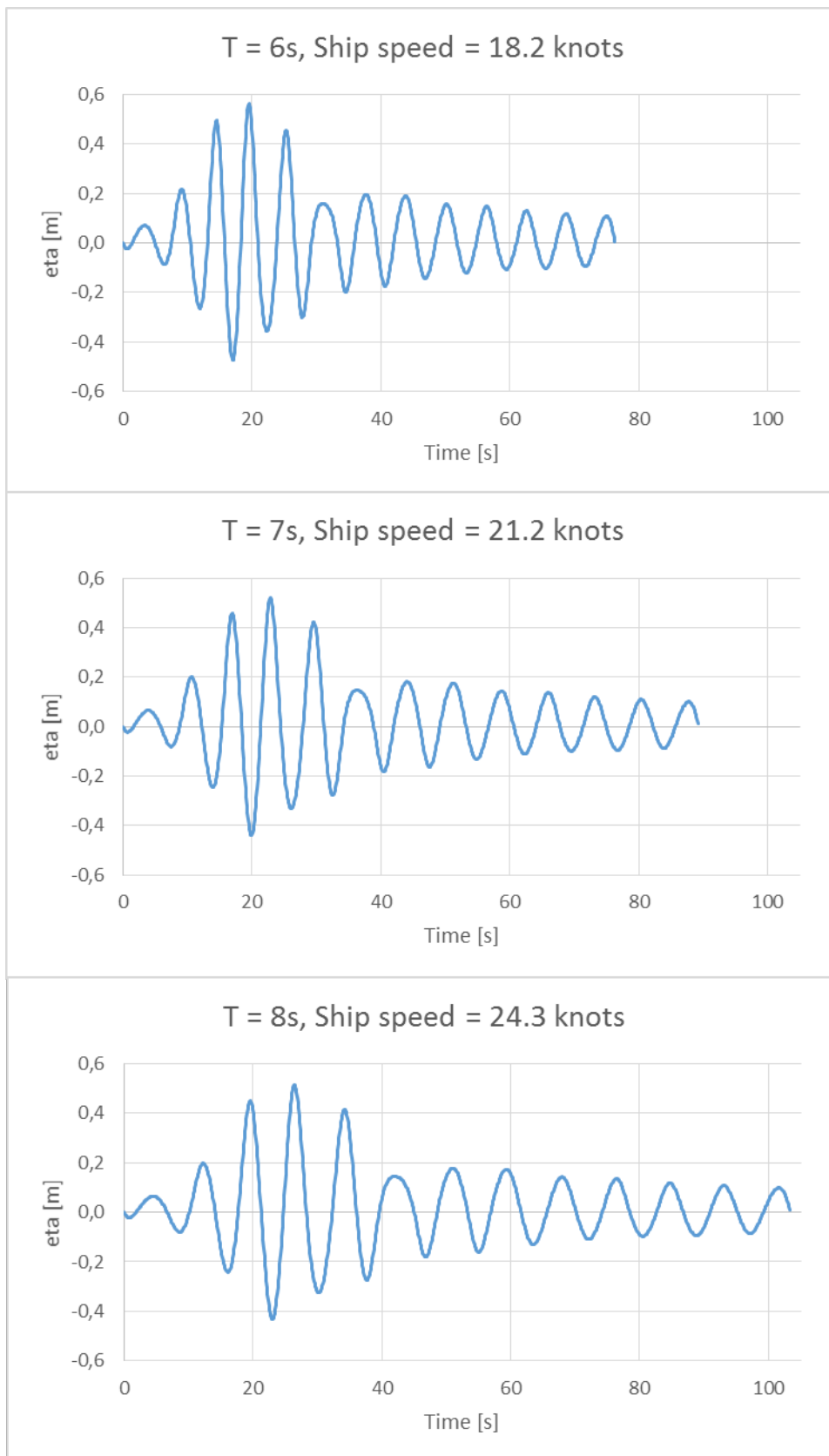


Figure 4 Vessel induced waves.

2 Wind

The input for wind loading is done following N400 [1] and NS-EN 1991-1-4: 2005+NA [9]. Measurement and simulations are used to validate the recommendations in N400, and as a supplement to give more detailed information about the wind field when necessary. For more information, see [10] for wind observations and [11] for wind simulations.

2.1 Return periods

The wind speed, V , in Table 12 is valid for 10 m height. For extrapolation to higher levels, see 2.1.3. The values given are in accordance with the wind climate described in N400 with a roughness length $z_0 = 0.01$ and a terrain factor $k_T = 0.17$. To find the 1 hour mean the 10 min mean is reduced by 7% [11].

Return period	Wind speed, V [m/s] 1 h mean	Wind speed, V [m/s] 10 min mean
1	21.4	22.9
10	25.8	27.6
50	28.5	30.5
100	29.6	31.7
10 000	35.9	38.4

Table 12 1 hour and 10 minutes mean wind with given return periods.

A summer reduction (May-Aug) of 0.8 can be used for all heights, return periods and averaging periods.

2.1.1 Sectoral extremes

The reduction factors in Table 13 can be multiplied by the wind speeds from Table 12 to find the sectoral extremes. The reduction factors are calculated from wind simulations [12].

The different sectors refer to the direction from which the wind is coming. $0^\circ/360^\circ$ means wind coming from the north, 90° coming from the east, 180° from the south and 270° from the west.

Sectors	Reduction coeff.
$0^\circ-75^\circ$	0.7
$75^\circ-225^\circ$	0.85
$225^\circ-255^\circ$	0.9
$255^\circ-285^\circ$	1.0
$285^\circ-345^\circ$	1.0
$345^\circ-360^\circ$	0.7

Table 13 Directional reduction coefficients.

2.1.2 Distribution along the bridge

The mean wind speed can be assumed to have the following distributions along the bridge axis [12]:

- 1) Constant
- 2) Linearly varying from 0,6 x V at one end to V on the other.
- 3) Linearly varying from 0,8 x V at one end to V in the middle to 0,8 on the other end

2.1.3 Wind profile

The wind profile for 1 hour mean can be found following N400

$$V(z) = C_r(z) * 24.3$$

where

$$C_r = k_T * \ln\left(\frac{z}{z_0}\right)$$

with $z_0 = 0.01$ and $k_T = 0.17$.

10 min mean is found by multiplying $V(z)$ by 1.07.

For episodes with strong winds the simulations show a steeper profile than what is given in N400, hence the profile recommended seems to be a conservative choice above 50 meters. More information about the wind profile is given in [12].

2.2 Turbulence intensity

Sector 0°-150° and 210°-360°

The turbulence can be assumed to follow the equation given in NS-EN 1991-1-4: 2005+NA

$$I_u = \frac{k_{tt}}{\ln\left(\frac{z}{z_0}\right)}$$

where $k_{tt} = 1.0$ and $z_0 = 0.01$ and z is the height.

This is in agreement with measurements which give an average longitudinal turbulence intensity of 0.112 for $U > 12$ m/s in 50 meters height. The lateral and the vertical turbulence components I_v and I_w found from the measurements [10] are

$$\begin{bmatrix} I_v \\ I_w \end{bmatrix} = \begin{bmatrix} 0.84 \\ 0.60 \end{bmatrix} I_u$$

Sector 150°-210°

Wind coming from the south is very turbulent on the southern side of the fjord. Measurements show a turbulence intensity of 30% for strong winds in 50 meter height. The measurements are representative for the conditions at the location of the southern tower. The turbulence intensity can be assumed to decrease linearly from 30% to 17% in the north.

Analysis of turbulence intensities from wind simulations in 200 meter height shows only small variations across the fjord, and is calculated to be 15% for strong winds.

Sector/ Height above sea	150°-210° Turbulence intensity
10-50	Linearly decreasing from 30% at southern tower to 17% in the north
200	15%

Table 14 Turbulence intensities for southerly winds.

2.3 Power spectral density of wind turbulence

The frequency distribution of the turbulence components in all three directions and the statistical dependence between the turbulence components at two points at a given frequency is described following N400.

One point spectra $S_i(n)$ is given by

$$\frac{nS_i}{\sigma_i^2} = \frac{A_i \hat{n}_i}{(1+1.5A_i \hat{n}_i)^{5/3}} \text{ for } i = u, v, w$$

where n is the frequency, u, v, w is the turbulence components, A_i is the spectral density coefficients (Table 15), σ_i is the standard deviation of the turbulence components and

$$\hat{n}_i = \frac{n^x L_i(z)}{V(z)}$$

where $V(z)$ is the 10 minute wind speed in height z (Table 12 and section 2.1.3) and $^x L_i(z)$ is the turbulent length scales (Table 15).

The normalized cospectra $S_{i_1 i_2}$ for separation normal to the main flow, horizontal (y) or vertical (z), is given by

$$\frac{\text{RE} [S_{i_1 i_2}(n, \Delta s_j)]}{\sqrt{S_{i_1}(n) \cdot S_{i_2}(n)}} = \exp\left(-C_{ij} \frac{n \Delta s_j}{V(z)}\right)$$

where Δs_j is the horizontal or vertical distance between points of interest,

$$i_1, i_2 = u, v, w$$

$$j = y, z$$

and C_{ij} is given in Table 15.

Measurements in the Bjørnafjord are carried out with a sampling frequency of 10 Hz. Analysis of turbulence scale parameters are calculated from measurements in 50 m height, with periods of 20-minutes with easterly wind and wind speed exceeding 10 m/s [13]. The parameters are given in Table 15 as percentiles p10, p50 and p90.

Parameter	N400	P10	P50	P90
xL_u	162 m	108 m	232 m	586 m
yL_u	40.5 m	50 m	141 m	472 m
zL_u	13.5 m	21 m	40 m	81 m
xL_v	12.5 m	X	X	X
yL_v	12.5 m	X	X	X
zL_v	4.2 m	X	X	X
xL_w	4.2 m	X	X	X
yL_w	2.8 m	X	X	X
zL_w	2.8 m	X	X	X
A_u	6.8	3.9	7.3	16.3
A_v	9.4	5.6	13.3	32.5
A_w	9.4	7.7	12.3	18.2
C_{uy}	10.0	6.4	8.0	10.8
C_{uz}	10.0	8.3	11.5	17.6
C_{vy}	6.5	3.0	3.8	4.9
C_{vz}	6.5	6.0	8.8	16.5
C_{wy}	6.5	4.5	5.8	8.3
C_{wz}	3.0	2.8	3.7	5.7

Table 15 Turbulence scale parameters for the Bjørnafjord (50 m above ground level).

3 Current

According to N400 [1], chapter 13.12.3.3, the loading due to the currents should be based on information from measured and simulated current profiles from the fjord. For Bjørnafjorden almost 2.5 years of current measurements are available from 5 different stations. One of the locations is measuring almost the whole water column. The rest is focusing on the upper 50 m of the water column. The ADCP instruments used in the monitoring campaign, however, have limitations when it comes to measuring the important upper 5 m of the water column. Therefore numerical simulations are necessary. For more information about the current measurement program, see [14].

22 year of hindcast current data from Bjørnafjorden are available from the Norwegian Coastal Model (NorKyst800) run by the Institute of Marine Research. The model data has 800 m horizontal resolution. For more information about the model and the model setup, see [15]. In addition, a higher resolution model, NorFjord160, is set up for the Hardangerfjord, where also Bjørnafjorden is a part of the model domain. The model has 160 m horizontal resolution and been used to produce high-resolution current data for Bjørnafjorden for almost 2 years that coincide with the measured data. For a validation and comparison between measured and model results produced by the two models described above for the Hardangerfjord, see [16].

A validation of the model results of NorKyst800 and NorFjord160 has been carried out with the use of the measured data from Bjørnafjorden, see [17]. The short 160 m current data series is then extrapolated to the long term period of NorKyst800. The result is then used to estimate extreme sea currents and directions, see Table 16 and Table 18. For further information about the methods and results, see [18]. The current directions refer to the direction towards which the current is flowing.

The extreme values of hourly sea current (m/s) for four different locations (marked S1-S4) at the planned bridge crossing is found in Table 16 with return periods of 10, 50 and 100 years. Linear interpolation can be used between depths and the locations. The distances from the shore in the south (LS) to each location of the crossing are given in Table 17. Figure 5 shows the locations (S1-S4) and

the northern (LN) and southern (LS) shore in Table 17. Table 16 and Table 18 are going to be used when computing the current effect on the bridge pontoons.

Return period [year]	Depth [m]	S1	S2	S3	S4
10	1.5	1.49	1.45	1.27	1.30
	5.0	1.26	1.55	1.26	1.55
	10.0	1.23	1.18	1.08	1.14
	15.0	0.96	0.99	1.11	1.29
50	1.5	1.68	1.63	1.46	1.54
	5.0	1.45	1.85	1.51	1.94
	10.0	1.39	1.34	1.24	1.38
	15.0	1.15	1.14	1.31	1.54
100	1.5	1.76	1.71	1.54	1.64
	5.0	1.53	1.97	1.62	2.11
	10.0	1.46	1.40	1.31	1.48
	15.0	1.23	1.21	1.39	1.65

Table 16 Extreme values of hourly sea current [m/s] at the Bjørnafjord crossing for four depths. 1 year extreme values may be found by multiplying the 100 year values with a factor 0.64, and for calculating the 10 000 years the value 1.36 may be used.

LS	S4	S3	S2	S1	LN
0	700	1900	2900	3600	4900

Table 17 Distance from land at the southern shore (LS) to each location given in Table 16 in meter. LN marks the northern shore.

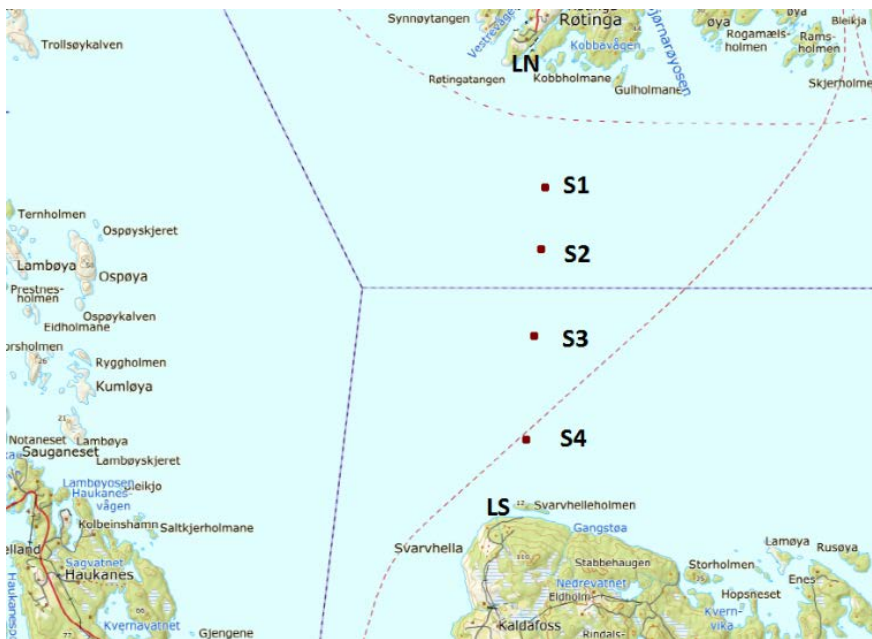


Figure 5 The locations of the stations (S1-S4) and northern and southern shore, LN and LS respectively.

The sectoral extreme speeds of the planned bridge crossing can be found by multiplying the reduction factors in Table 18 for four different depths with Table 16 for the corresponding depths. This is going to be used when computing the sectoral current effect on the bridge pontoons.

Depth [m]	Location	N	NE	E	SE	S	SW	W	NW
1.5	S1	0.97	1.00	0.55	0.40	0.44	0.45	0.69	0.41
	S2	0.87	1.00	0.61	0.44	0.48	0.53	0.66	0.39
	S3	0.76	1.00	0.58	0.53	0.54	0.50	0.69	0.41
	S4	0.63	0.89	0.99	0.56	0.47	0.72	0.56	0.41
5.0	S1	0.63	1.00	0.57	0.44	0.37	0.32	0.51	0.47
	S2	0.50	1.00	0.49	0.40	0.34	0.29	0.49	0.33
	S3	0.52	1.00	0.56	0.40	0.26	0.39	0.51	0.35
	S4	0.21	0.47	1.00	0.60	0.42	0.54	0.49	0.30
10.0	S1	0.51	1.00	0.50	0.33	0.27	0.22	0.33	0.43
	S2	0.53	1.00	0.50	0.42	0.26	0.26	0.38	0.39
	S3	0.49	1.00	0.60	0.45	0.31	0.30	0.48	0.41
	S4	0.33	0.36	1.00	0.78	0.36	0.35	0.43	0.46
15.0	S1	0.74	1.00	0.70	0.41	0.30	0.30	0.37	0.48
	S2	0.69	1.00	0.73	0.36	0.33	0.35	0.39	0.39
	S3	0.70	1.00	0.84	0.37	0.33	0.28	0.34	0.32
	S4	0.67	0.64	1.00	0.79	0.40	0.33	0.37	0.22

Table 18 Relative sector speed during extreme conditions for 8 sectors at the Bjørnafjorden crossing for four depths.

In [18] the focus were on the upper 15 m of the water column. Mean estimates of the extreme currents for all depths are found in Table 19. A brief description of how these extreme values are calculated is given in [19]. These extreme currents should be used when calculating the current loading on the anchoring. Linear interpolation can be used between the depths.

Depth [m]	Return period 10 year	Return period 50 year	Return period 100 year
1.0	1.50	1.66	1.73
2.0	1.45	1.64	1.72
3.0	1.41	1.61	1.70
4.0	1.37	1.58	1.67
5.0	1.33	1.54	1.63
6.0	1.29	1.51	1.60
7.0	1.24	1.46	1.55
8.0	1.20	1.42	1.50
9.0	1.16	1.37	1.45
10.0	1.13	1.32	1.40
15.0	1.03	1.21	1.28
20.0	0.96	1.12	1.18
25.0	0.92	1.06	1.12
30.0	0.87	1.00	1.06
35.0	0.84	0.98	1.03
40.0	0.78	0.89	0.94
45.0	0.73	0.84	0.89
50.0	0.70	0.82	0.87
60.0	0.63	0.73	0.78
70.0	0.57	0.66	0.69
80.0	0.54	0.63	0.66
90.0	0.51	0.60	0.65
100.0	0.48	0.57	0.61
125.0	0.45	0.52	0.55
150.0	0.46	0.55	0.59
175.0	0.48	0.59	0.63
200.0	0.40	0.49	0.53
225.0	0.31	0.36	0.39
250.0	0.27	0.32	0.34
300.0	0.30	0.34	0.36

Table 19. Mean extreme values of hourly sea current [m/s] at the Bjørnafjorden crossing for different depths. For depths more than 300 m the return values of 300 m can be used. 1 year extreme values may be found by multiplying the 50 year values with a factor 0.65, and for calculating the 10 000 years the value 1.3 may be used.

The effect of internal waves is investigated in [20]. The work show that the strongest internal waves that can occur will occur in summer due to the thin interface between the upper and lower layer and large upper layer which allows for larger amplitude internal waves. This is in agreement with [21] and shows that the most extreme internal waves does not occur at the same time as the most extreme winds (which occur in the winter time).

[20] concludes that internal waves can occur in Bjørnafjorden, but the strength of the extreme currents due to internal waves will be weaker than the currents originating from extreme wind events. In the extreme value analysis, the model results will contain internal wave events, wind generated events and

a combination of these. The extreme value analysis as presented here, therefore, capture the relevant extreme events in the Bjørnafjord without adding extra unnecessary conservatism.

4 Water level variations

The water level variation is defined as an astronomical component and a surge component combined. The surge component includes effects from low/high atmospheric pressure and storm surge. The astronomical component is independent of the environmental conditions, whereas the surge component is governed by the atmospheric conditions. Since the confidence on the two components vary, that is, astronomical tide values are lot more predictable than the surge components are, appropriate safety factors can be applied separately on each component during further design.

The reference level for the tidal amplitudes in Table 20 and the water level in Table 21 is chart datum (LAT). The values are based on data from Kartverket [22].

Tidal amplitudes [m]	
Lowest Astronomical Tide (LAT)	0.00
Mean Low Water (MLW)	0.39
Mean Sea Level (MSL)	0.77
Mean high water (MHW)	1.15
Highest Astronomical Tide(HAT)	1.53
NN 1954	0.88
NN 2000	0.97

Table 20. Tidal amplitudes.

The water level for different return periods may be taken from Table 21.

Return periods [years]	Highest water level [m]	Lowest water level [m]
1	1,81	-0,20
10	1,97	-0,30
100	2,10	-0,50
10000	2,50	-0,65

Table 21. Water level related to return periods relative to LAT.

The surge component (air pressure effect, storm surge etc) may for simplicity and until more reliable data are collected be taken as the difference between the values in Table 21 and MSL.

The mean water level shall be increased by 0.74 m due to climate change where this is unfavorable. [23]. This number includes the effect of land elevation rise. For more information on climate change implication refer to section 7.

5 Water density variations

From the 2.5 years of measurements of salinity and temperature [14] it is found that the minimum density is 1009.7 and the maximum density is 1026.1 kg/m³ at 2 m depth in the center of the Bjørnafjord. Densities less than 1015 kg/m³ occurs very rare and are most likely connected to events where large volumes of fresh water enter the fjord system and propagate as pulses. For the measured period the density is most of the time within the range 1020-1025 kg/m³, see [24]. To convert from

salinity and temperature measurements to density, the UNESCO 1983 algorithms have been used [25]. For further information about the measured density, see the discussions in [24].

Chapter 13.12.2.2 in N400 gives recommendations concerning the choice of water density in lack of measurements. Our measured values are within the range recommended here.

6 Temperature

6.1 Air temperature

According to NS-EN 1991-1-5:2003+ NA:2008 the lower and upper representative air temperature (T_{\min} and T_{\max}) is taken from the isotherm map in attachment NA.A.2. To narrow the given range additionally, an analysis of measurements and model results have been performed [26] leading to the values given in Table 22.

Return period 50 years	Temperature [degree Celsius]
Maximum	32
Minimum	-15

Table 22. Maximum and minimum temperature with 50 years return period.

6.2 Sea temperature

The sea temperature data is taken from the model results produced by the setup described in [15]. The validation of the model results and comparison with the measured data is described in [27]. The absolute range of the sea temperature at 2 m depth is from 2.1 to 20.6 degree Celsius. The values in Table 23 are computed from modelled data taken at 2 m depth. In N400 the return period for sea temperature is not explicitly given, but for consistency with the air temperature a return period of 50 years is calculated. NORSOK N-003:2017 uses extreme sea and air temperature with an annual probability of 10⁻². For other return periods, refer to [27].

Return period 50 years	Temperature [degree Celsius]
Maximum	21.5
Minimum	1.3

Table 23 Maximum and minimum sea temperature with 50 years return period.

7 Climate change

The future wind, wave and current conditions might change due to climate change. The lifetime of the bridge exceeds 100 years and climate change should be accounted for. Future metocean conditions can be predicted by running global climate models in combination with regional downscaling and numerical wind and wave models. However, the accuracy in the predictions are at the present not sufficient to quantify the consequence on the extreme conditions [2].

In lack of detailed documentation, the recommendations stated in NORSOK N-003:2017 Action and Action Effects [2] may be used:

- extreme significant wave heights: 4% increase on q-probability values;
- extreme wind speeds: 4% increase on q-probability values;

There is no recommendation for the extreme current speed in the NORSOK standard. We suggest using the same increase for current:

- extreme current speeds: 4% increase on q-probability values;

For sea level change, we recommend using the projected 95-percentile for the RCP8.5 scenario for the year of 2100. This value is obtained from Kartverket.no [28]:

- Projection for sea level in Bjørnafjorden 2100: + 74 cm

The report “Klima i Norge 2100” [23] gives an estimate for change in annual temperature of 2-3 degrees Celsius for Bjørnafjorden and surrounding areas. A trend analysis of measurements from Flesland shows that the max temperature might have increased by 1 degree Celsius from 1956 – 2017 [29]. Based on the limited information available we recommend

- an increase of 2 degrees Celsius on the maximum temperature
- no change for the minimum temperature

8 References

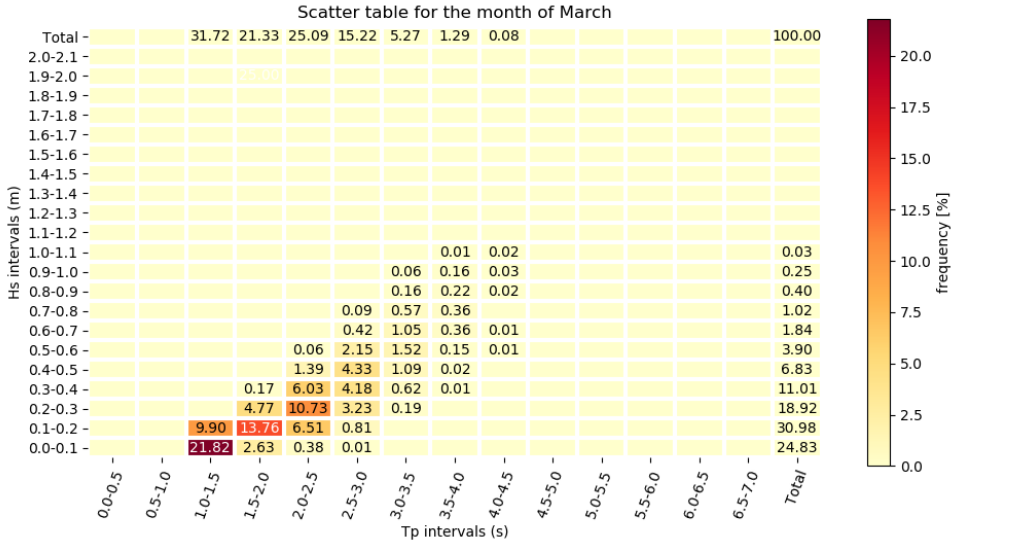
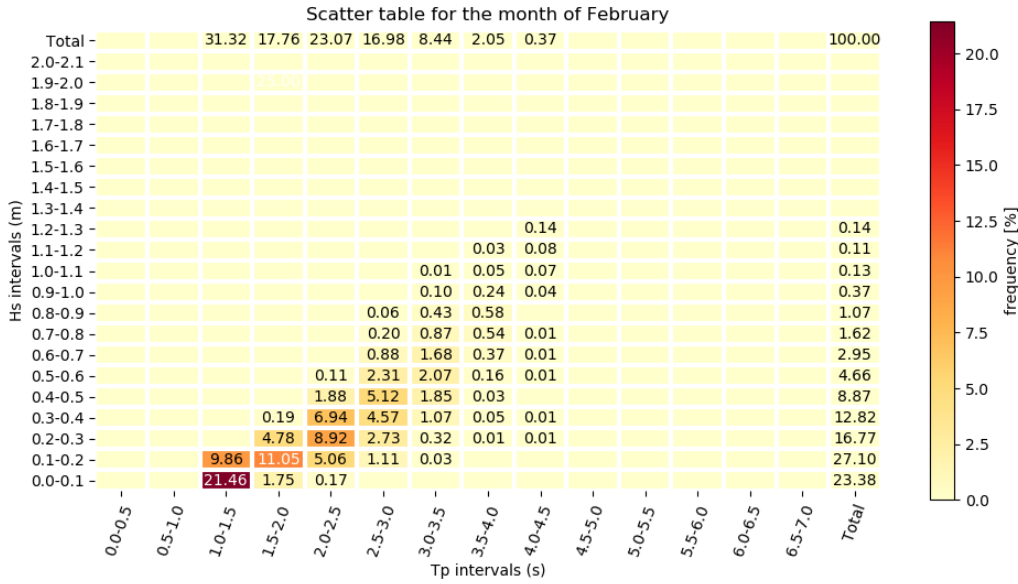
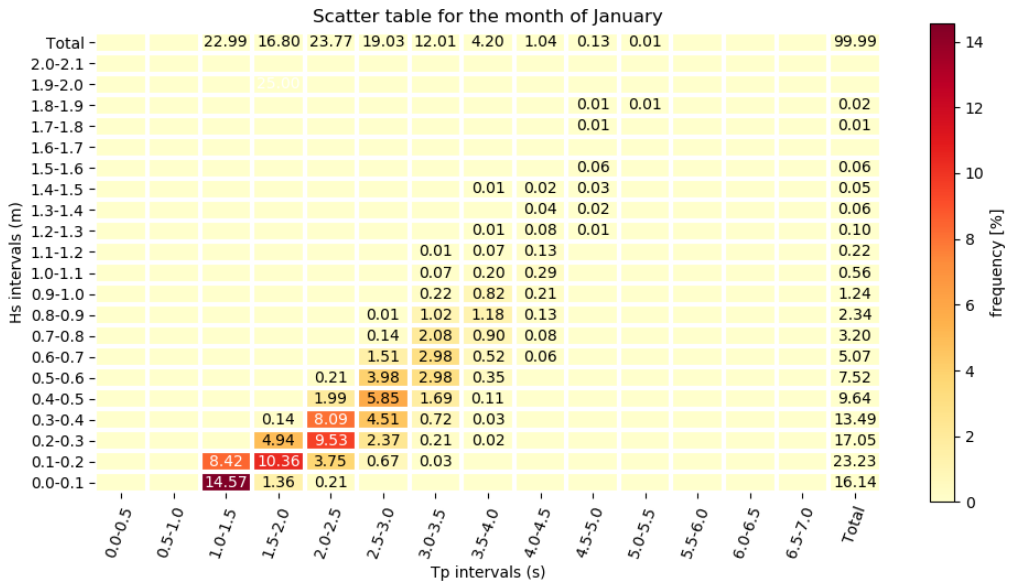
- [1] Statens Vegvesen, Vegdirektoratet, "Håndbok N400 Bruporsjektering, Prosjektering av bruer, ferjekaier og andre bærende konstruksjoner," 2015.
- [2] NORSOK Standard, "N-003:2017 Actions and action effects".
- [3] DNV, "Recommended practise DNV-RP-C205," April 2014.
- [4] O. J. Aarnes, "Wave Similation(15 years) report for Bjørnafjord," Meteorological Institute, Norway , 2018.
- [5] E. Svangstu, *SBJ-01-C4-SVV-01-TN-007 Sammenligning av modelleringsdata fra Meteorologisk Institutt SWAN mot måldata fra Bjørnafjorden*, Statens Vegvesen, 2018.
- [6] A. Lothe, "E39 Bjørnafjord Crossing, Design Wave Data, Assignment no: 514672, Doc. No. 1, Ver. 1," Norconsult, 21/06-2016.
- [7] E. Svangstu, "Technical Note, Wave conditions for phase 3," Norwegian Public Road Administration, December 2016.
- [8] DNV GL, "Loads and site conditions for wind turbines," DNV GL, 2016.
- [9] 2. EN-1991-1-4: 2005+NA, "Eurocode 1: Laster på konstruksjoner. Standard Norge," 2009.
- [10] Kjeller vindteknikk AS, "SBJ-01-C4-KJE-01-RE-106 Statusrapport vindmålinger Bjørnafjorden - pr mai 2018".
- [11] Kjeller vindteknikk AS, "SBJ-01-C4-KJE-01-TN-005 E39, Bjørnafjorden, Hordaland, Analysis og extreme wind at the fjord crossing," 2018.
- [12] H. K. Fuhr, "SBJ-01-C4-SVV-01-TN-006 Vind Bjørnafjorden - fase 5," 2018.
- [13] Kjeller vindteknikk, "SBJ-01-04-KJE-01-TN-004 Analysis of spectral coherence in observations if wind in meteorological masts," 2018.
- [14] DHI, "SBJ-01-C4-DHI-01-RE-106 Wave and current measurements in Bjørnafjorden, Hordaland, Norway. Half year report 7.," DHI, 2018.
- [15] Havforskningsinstituttet, "Fisken og Havet. 2011(2). NorKyst-800 Report No. 1. User Manual and technical descriptions," Havforskningsinstituttet, 2011.
- [16] I. Johnsen, Ø. Fiksen, A. D. Sandvik and L. Asplin, "Vertical salmon lice behaviour as a response to environmental conditions and its influence on regional dispersion in a fjord system," *Aquaculture Environment Interactions*, vol. 5, pp. 127-141, 2014.
- [17] Ø. Thiem, "SBJ-01-C4-SVV-01-RE-002 Sammenligning mellom målt og modellert strøm for Bjørnafjorden," Statens Vegvesen, 2018.
- [18] Kjeller Vindteknikk AS, "SBJ-01-C4-KJE-01-RE-001 Bjørnafjorden, Hordaland. Analysis of extreme sea current (KVT_2018_R092_KH E39)," Kjeller Vindteknikk, 2018.
- [19] Ø. Thiem, *SBJ-01-C4-SVV-01-TN-004 Kurvetilpasning for ekstremverdier på strøm for alle dyp, Bjørnafjorden*, Statens Vegvesen, 2018.
- [20] Norce AS, "SBJ-01-C4-NORC-01-RE-001 Modelling of extreme currents along the planned bridge in Bjørnafjorden," Norce, 2018.
- [21] L. Asplin, I. Johnsen, A. D. Sandvik, J. Albretsen, A. Sundfjord, J. Aure and K. K. Boxaspen, "Dispersion of salmon lice in the Hardangerfjord," *Marine Biology Research*, vol. 10, no. 3, pp. 216-225, 2014.
- [22] P. Jena, *SBJ-01-C4-SVV-01-TN-005 Comparision of Tidal water level data*, Statens Vegvesen, 2018.
- [23] I. Hanssen-Bauer, E. Førland, I. Haddeland, H. Hisdal, S. Mayer, A. Nesje, S. Sandven, S. A. A.B. Sandø and Å. B., "Klima i Norge 2100," 2018.
- [24] Ø. Thiem, *SBJ-01-C4-SVV-01-TN-001 Målte sjøtettheter Bjørnafjorden*, Statens Vegvesen, 2018.
- [25] P. Fofonoff and R. C. j. Millard, "Unesco 1983. Algorithms for computation of fundamental properties of sea water.," UNESCO technical papers on marine science, 1983.

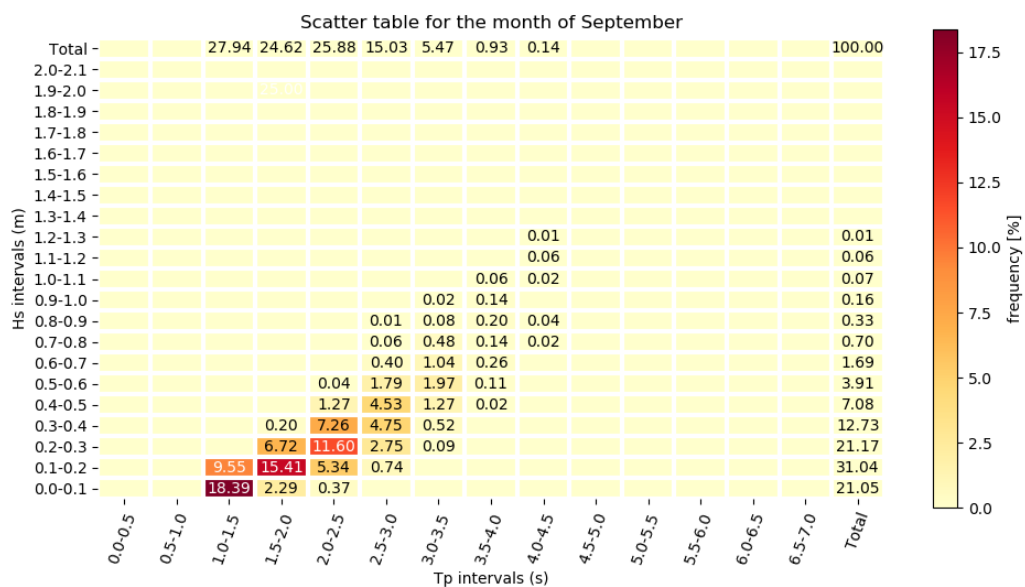
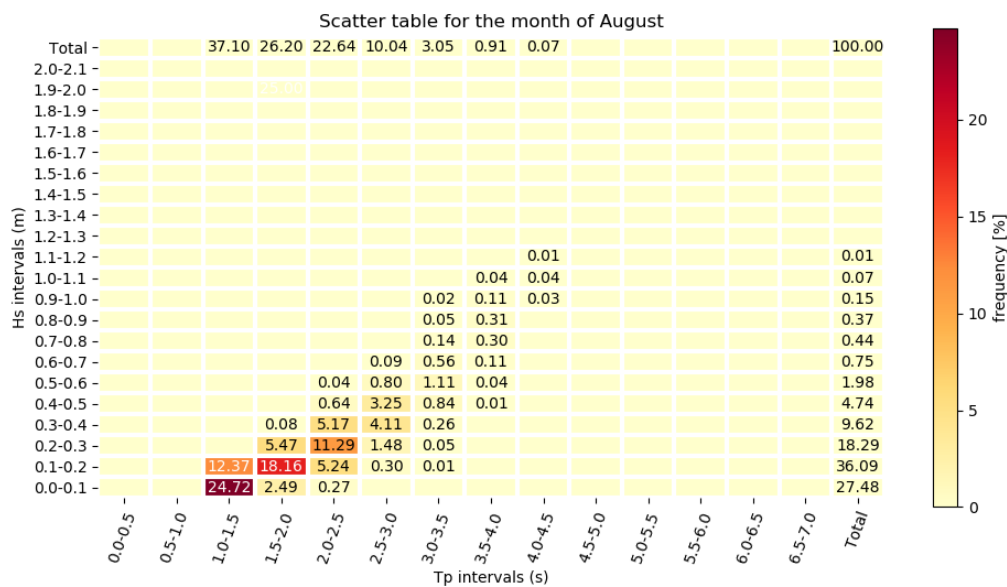
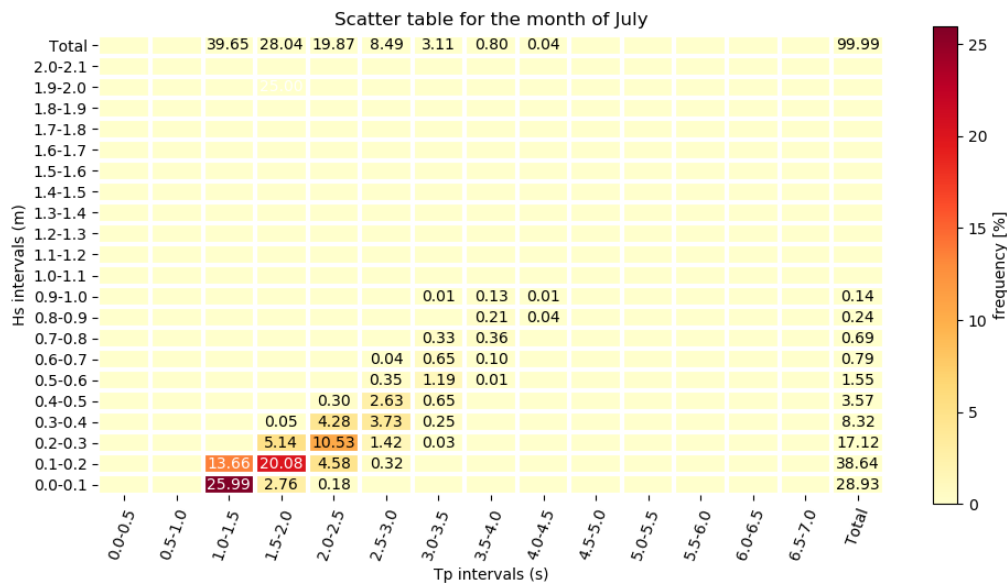
- [26] Ø. Thiem, *SBJ-01-C4-SVV-01-TN-003 Lufttemperaturer Bjørnafjorden*, Statens Vegvesen, 2018.
- [27] Ø. Thiem, *SBJ-01-C4-SVV-01-TN-002 Sjøtemperaturer Bjørnafjorden*, Statens Vegvesen, 2018.
- [28] kartverket, "<https://kartverket.no/sehavniva/sehavniva-lokasjonside/?cityid=77514&city=Bj%C3%B8rnafjorden#tab3>," [Online].
- [29] Kjeller vindteknikk, "Bjørnafjorden, Hordaland Temperaturanalyse," 2018.

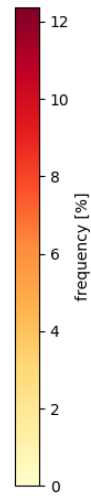
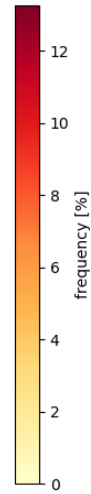
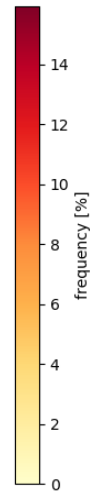
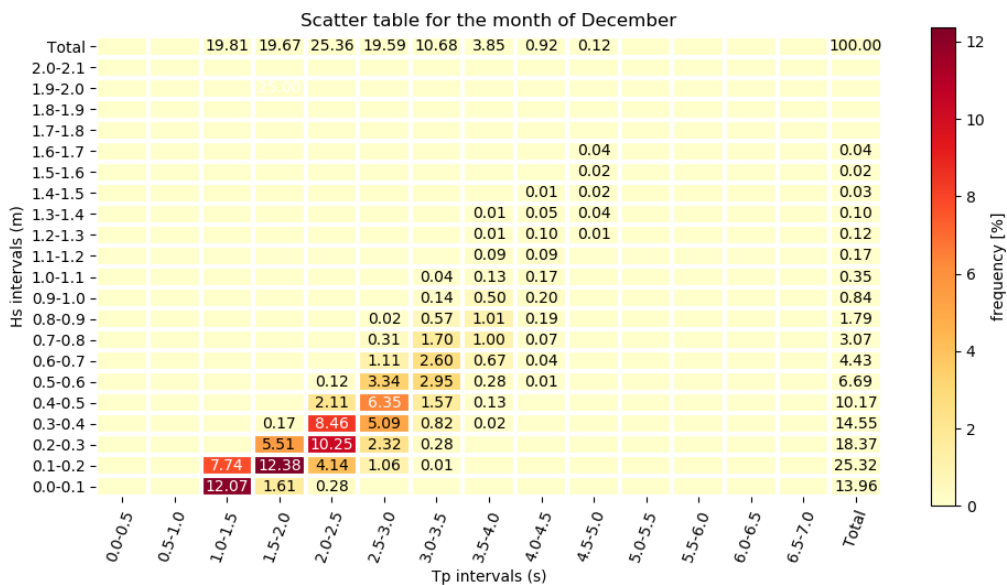
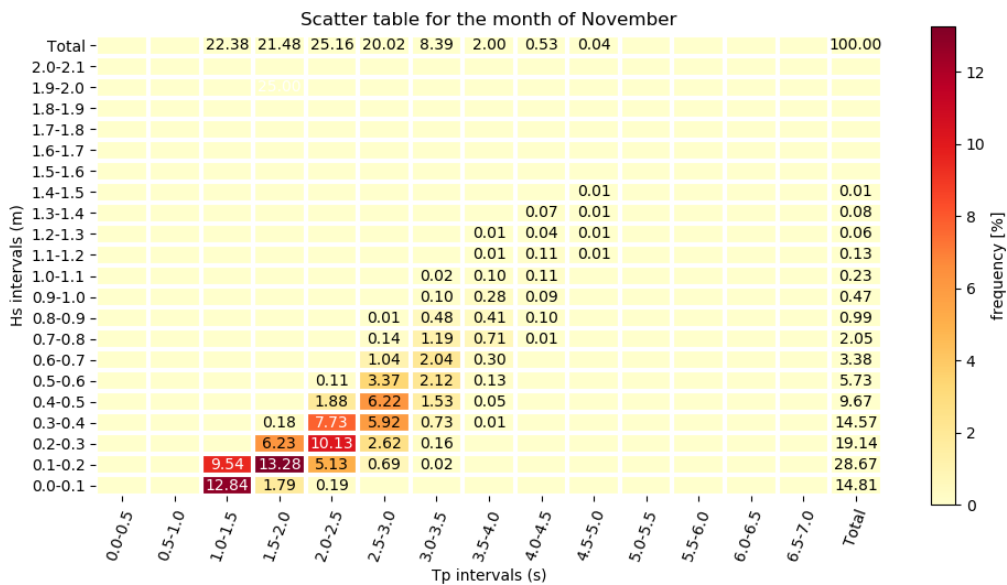
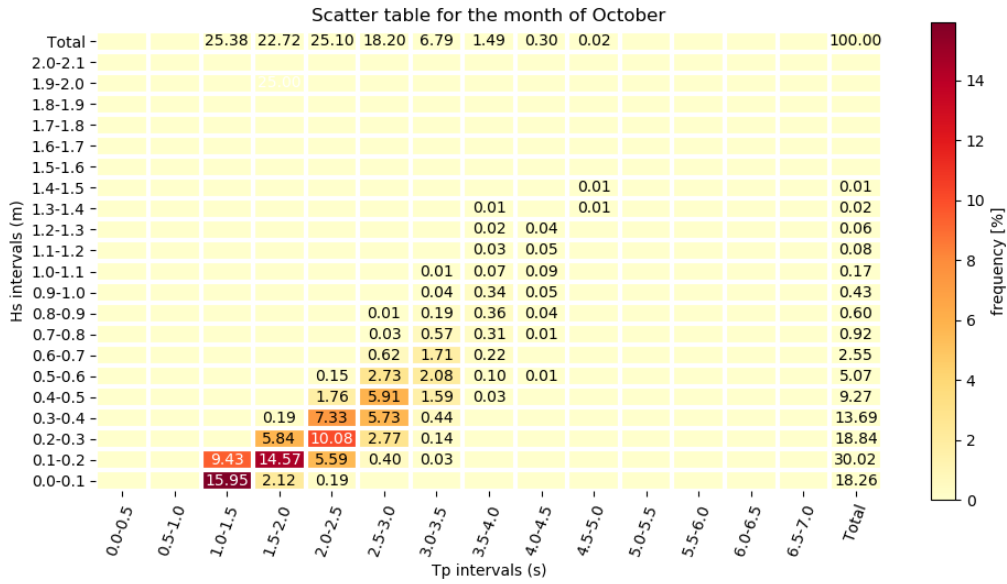
Appendix A

Wind Sea Scatter Diagrams and Hs Tp Contours

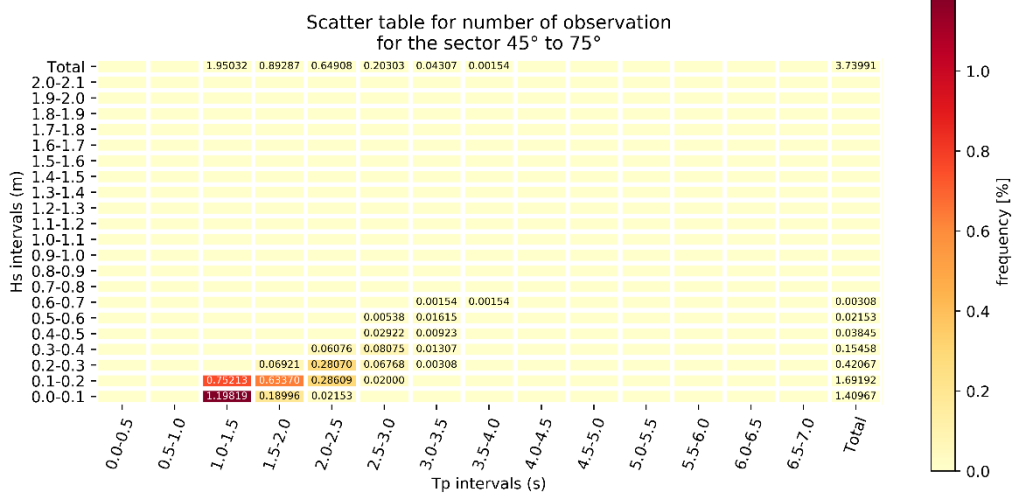
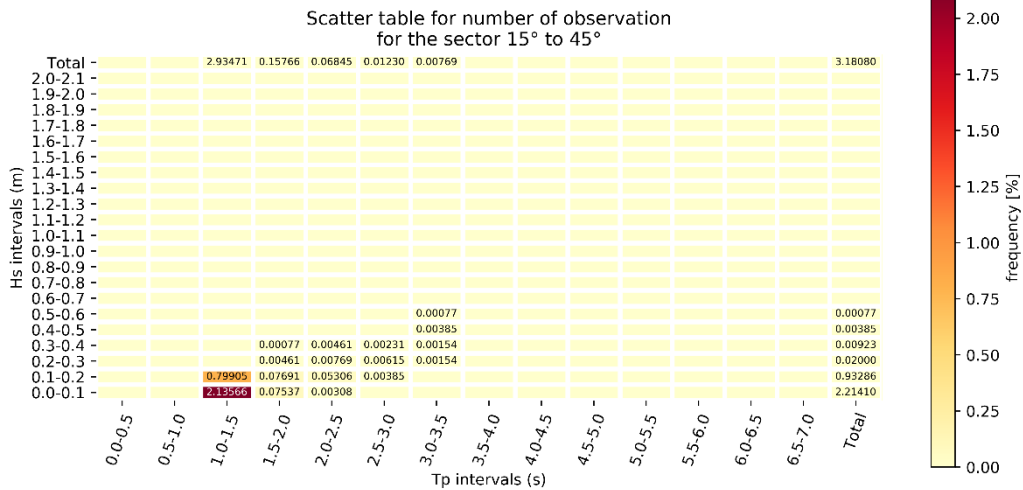
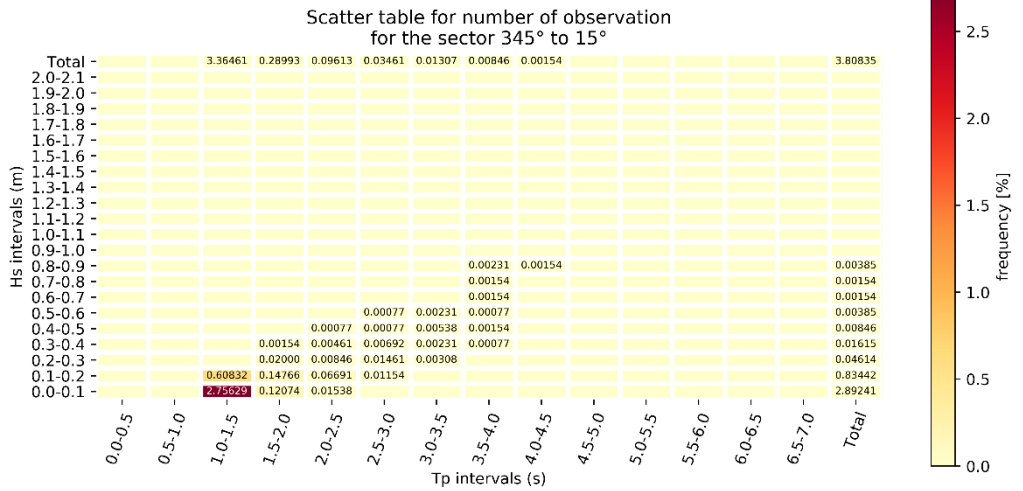
Season wise Scatter table for wind sea

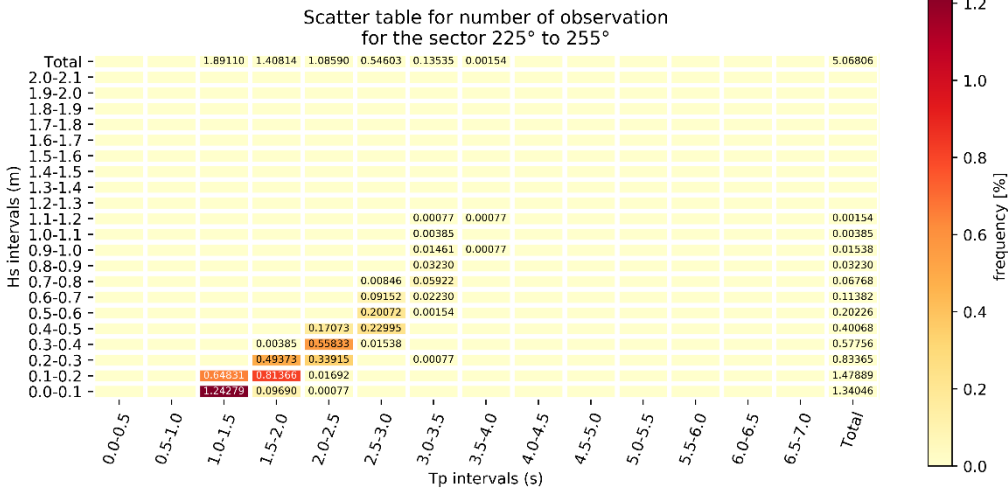
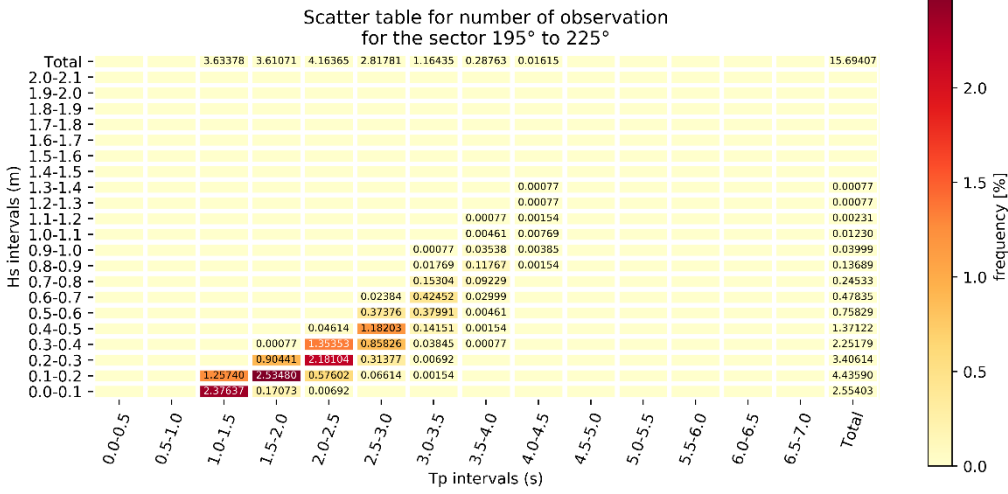
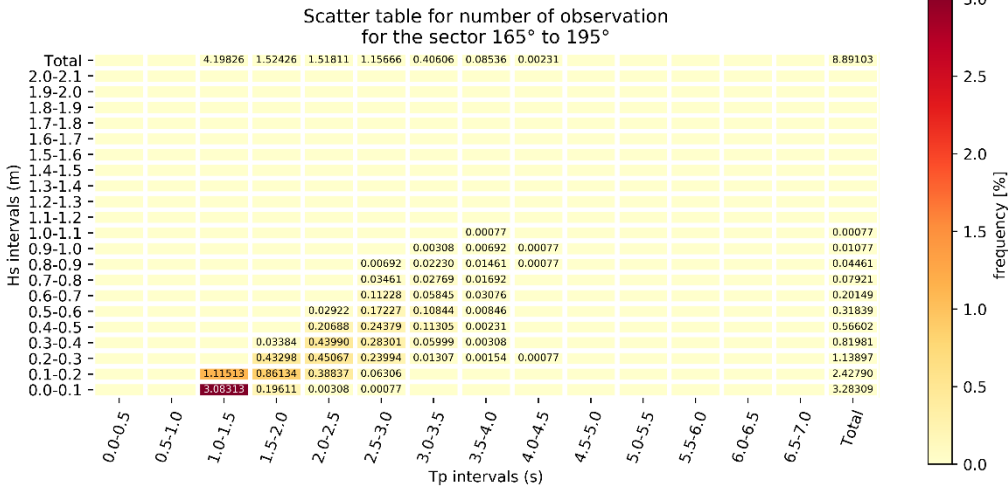




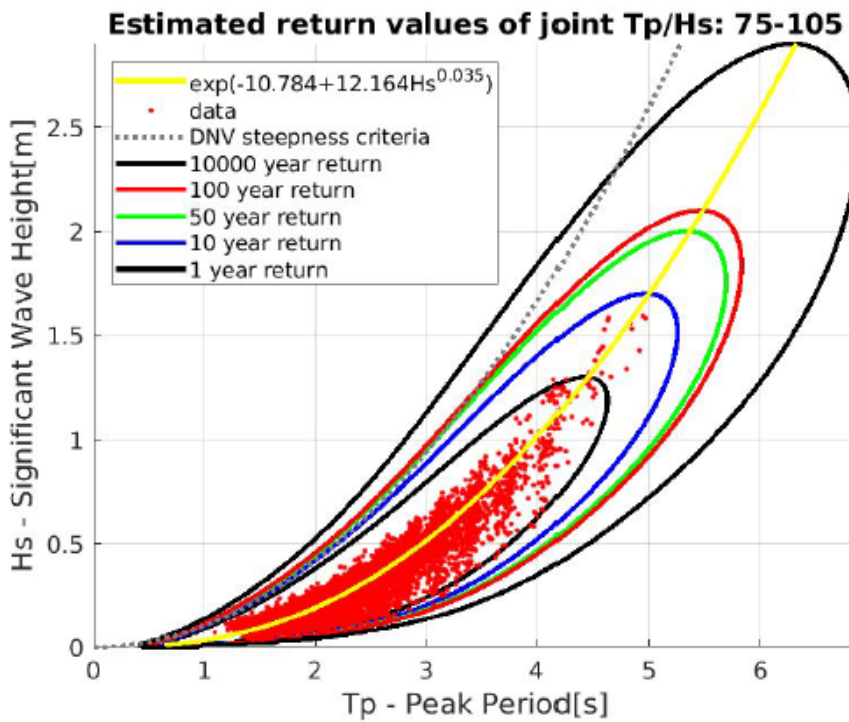
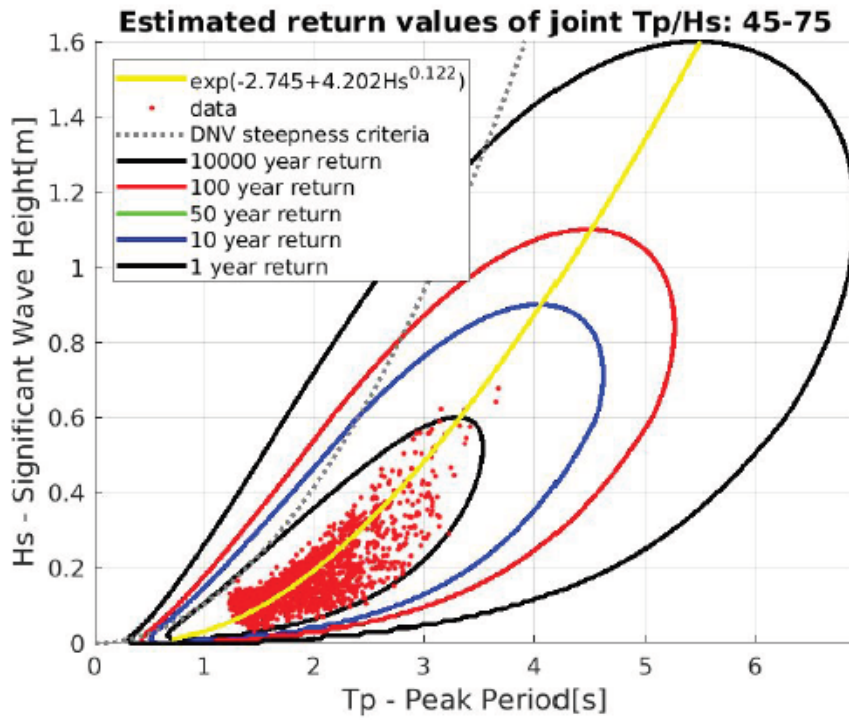


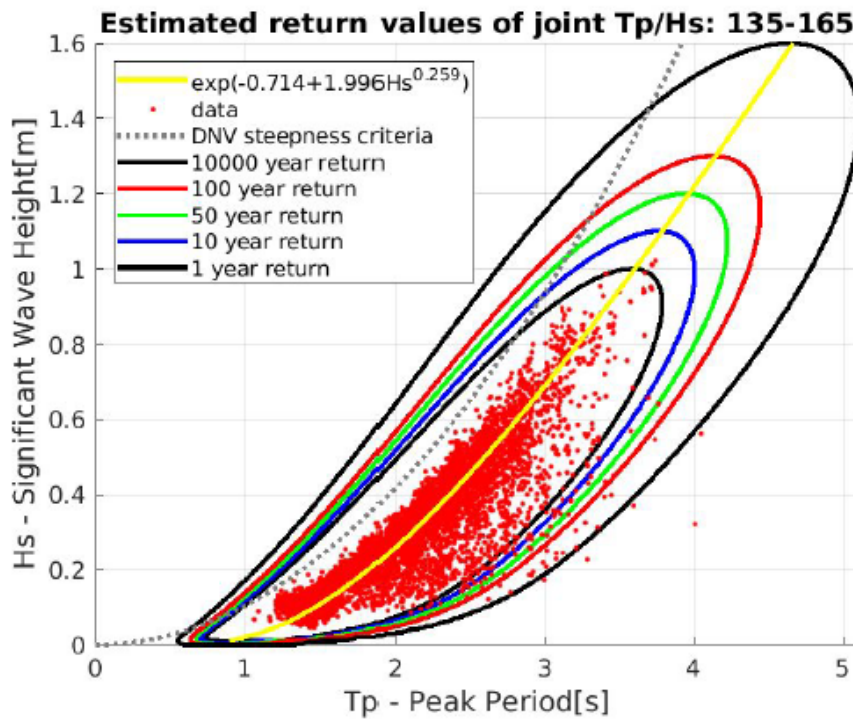
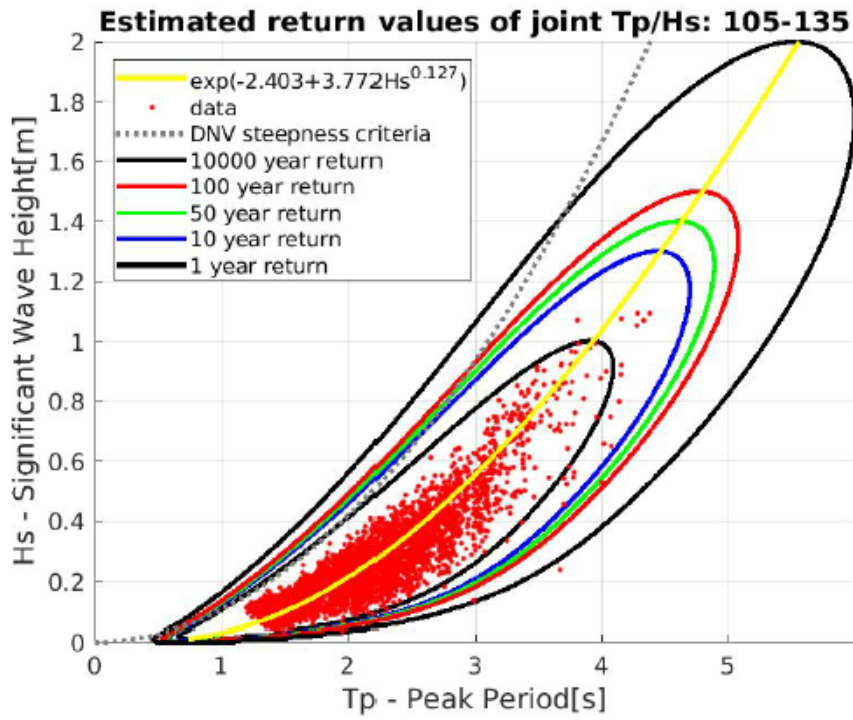
Sector wise scatter table for wind sea

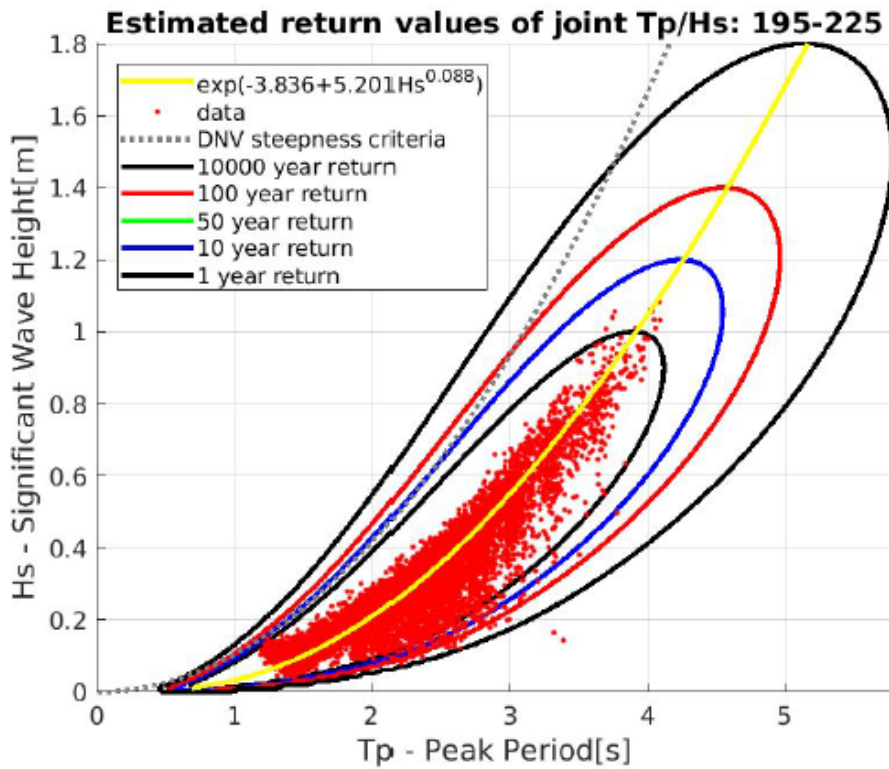
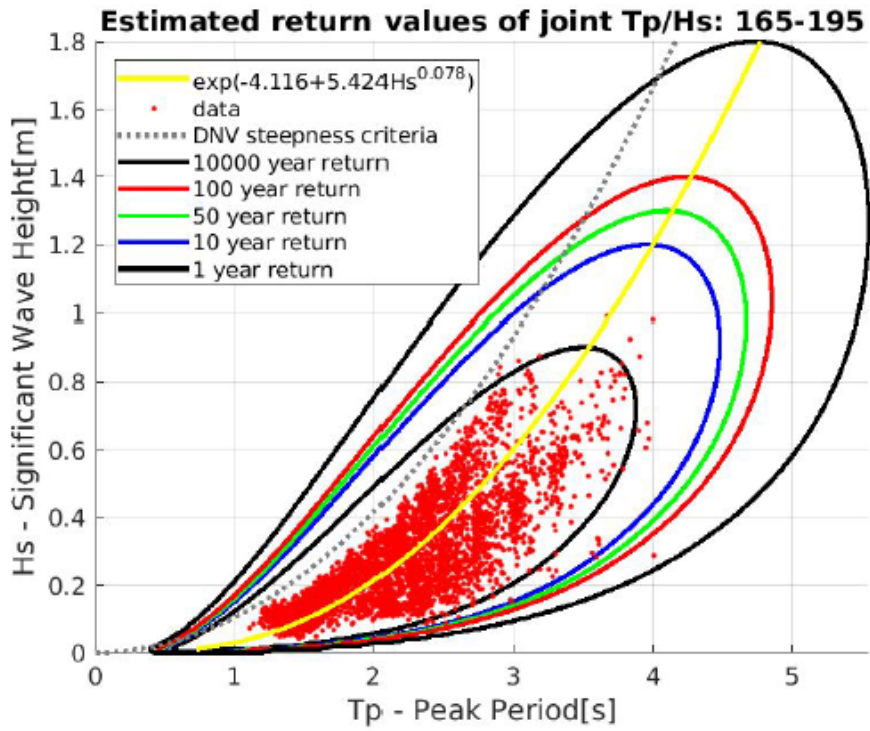


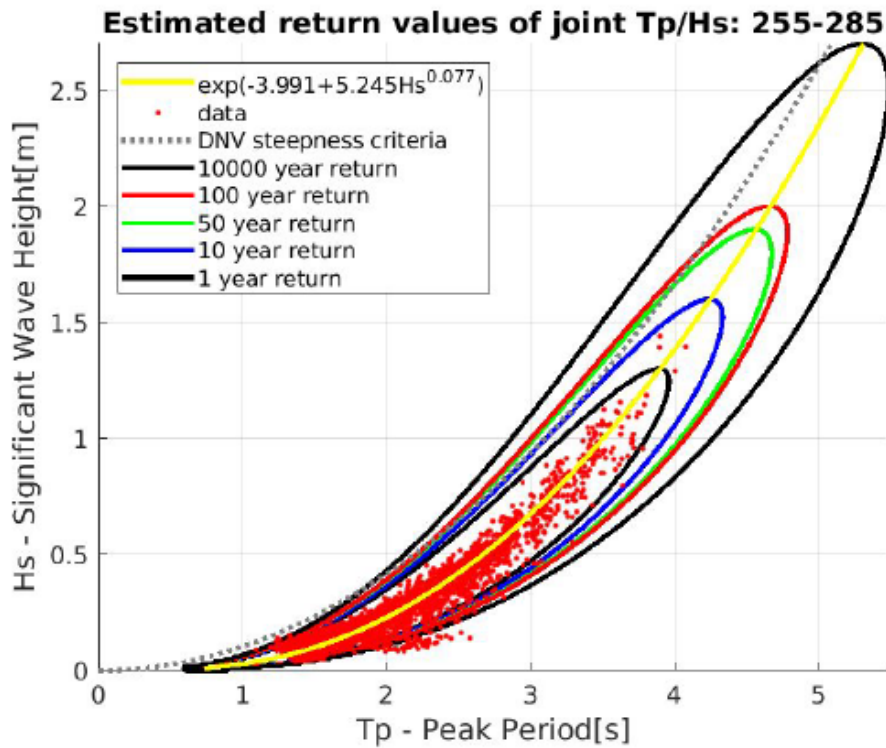
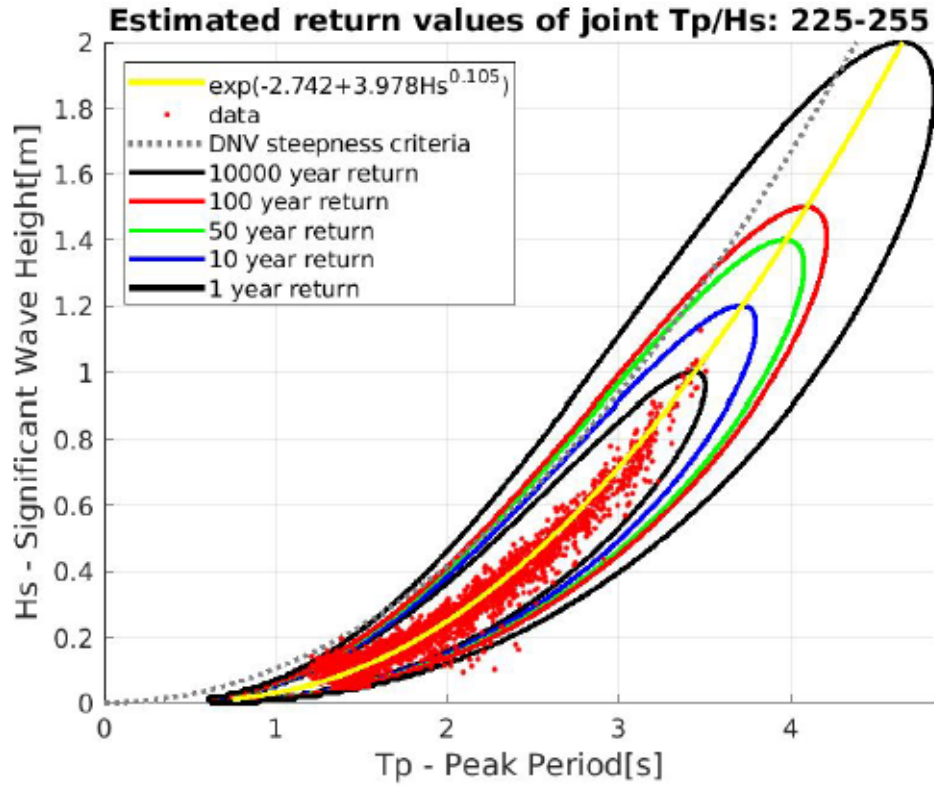


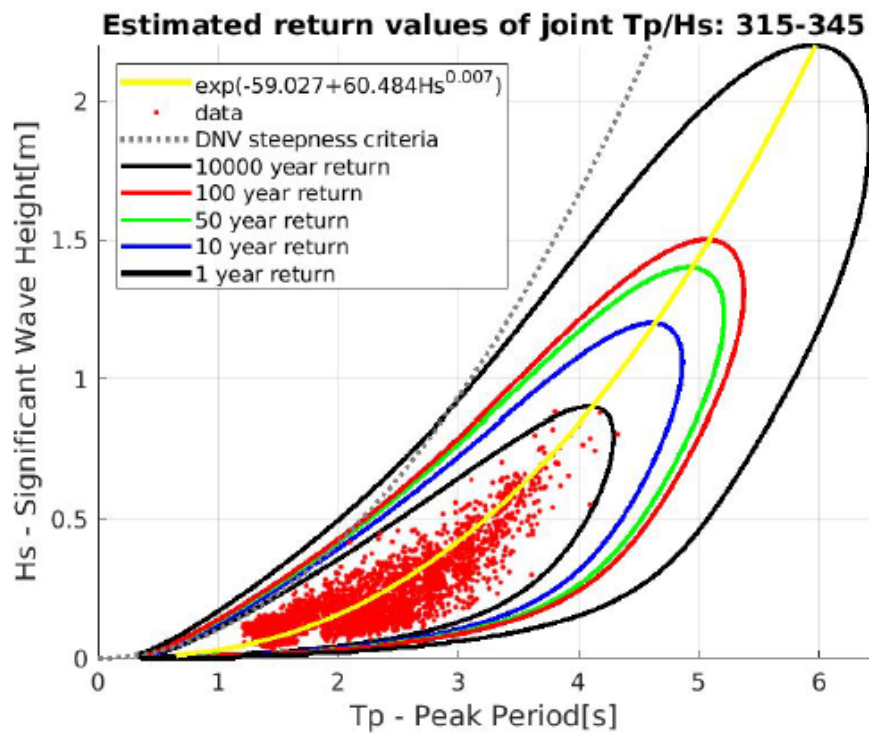
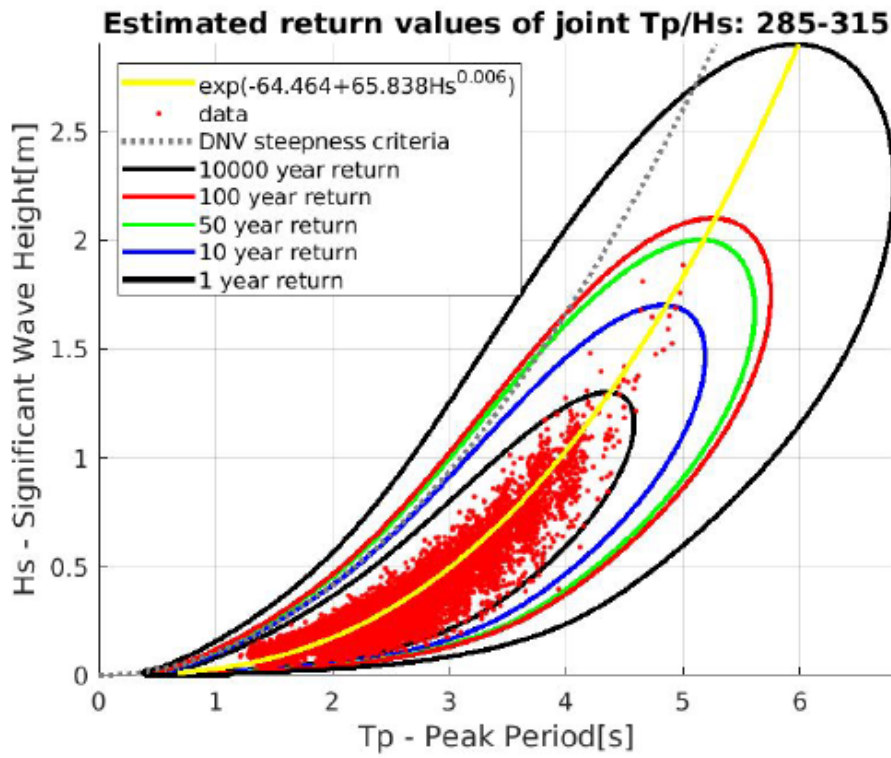
Sector-wise contour plots for wind sea











Appendix B

Swell Scatter Diagrams

Swell, Scatter diagram, March																						
Hm0	Tp																					
	<2	2 - 3	3 - 4	4 - 5	5 - 6	6 - 7	7 - 8	8 - 9	9 - 10	10 - 11	11 - 12	12 - 13	13 - 14	14 - 15	15 - 16	16 - 17	17 - 18	18 - 19	19 - 20	>20	Sum	
0,00	0,01	4,8422			0,0166	0,0518	0,0583	0,0666	0,1017	0,0971	0,0953	0,0860	0,0268	0,0222	0,0129	0,0028	0,0009				5,4814	
0,01	0,02				0,0185	0,0740	0,0749	0,0999	0,0860	0,0518	0,0888	0,0971	0,0925	0,0527	0,0213	0,0102	0,0018				0,7696	
0,02	0,03				0,0120	0,0416	0,0351	0,0416	0,0462	0,0805	0,0555	0,0740	0,0546	0,0277	0,0203	0,0074	0,0037	0,0018			0,5023	
0,03	0,04					0,0092	0,0462	0,0435	0,0176	0,0527	0,0583	0,0296	0,0379	0,0314	0,0213	0,0065					0,3543	
0,04	0,05						0,0499	0,0647	0,0407	0,0185	0,0250	0,0342	0,0111	0,0203	0,0176	0,0102	0,0018	0,0009			0,2951	
0,05	0,06						0,0231	0,0925	0,0777	0,0240	0,0092	0,0129	0,0148	0,0139	0,0083	0,0037	0,0028				0,2960	
0,06	0,07							0,0083	0,0573	0,0777	0,0388	0,0092	0,0018	0,0055	0,0065	0,0092	0,0037	0,0009			0,2248	
0,07	0,08							0,0009	0,0287	0,0499	0,0481	0,0185	0,0028	0,0009	0,0009	0,0018	0,0037				0,1563	
0,08	0,09								0,0055	0,0361	0,0601	0,0231	0,0028		0,0018			0,0009	0,0046		0,1350	
0,09	0,10								0,0009	0,0176	0,0388	0,0361	0,0009		0,0009		0,0009				0,0971	
0,10	0,11								0,0009	0,0231	0,0231	0,0028	0,0009								0,0509	
0,11	0,12								0,0018	0,0092	0,0185	0,0009									0,0305	
0,12	0,13								0,0018	0,0102	0,0120	0,0074	0,0009								0,0324	
0,13	0,14										0,0028	0,0074	0,0028		0,0009						0,0139	
0,14	0,15									0,0009	0,0102	0,0009	0,0009								0,0129	
0,15	0,16										0,0037	0,0166	0,0028								0,0231	
0,16	0,17										0,0009	0,0028	0,0028	0,0009							0,0074	
0,17	0,18										0,0009	0,0018									0,0028	
0,18	0,19											0,0018									0,0018	
0,19	0,20																				0,0000	
0,20	0,21																				0,0000	
0,21	0,22																				0,0000	
0,22	0,23																				0,0000	
Sum		4,8422	0,0000	0,0000	0,0000	0,0472	0,1767	0,2969	0,5013	0,5559	0,5541	0,4810	0,3940	0,2534	0,1794	0,1156	0,0573	0,0213	0,0111	0,0000	0,0000	8,4876
Swell, Scatter diagram, April																						
Hm0	Tp																					
	<2	2 - 3	3 - 4	4 - 5	5 - 6	6 - 7	7 - 8	8 - 9	9 - 10	10 - 11	11 - 12	12 - 13	13 - 14	14 - 15	15 - 16	16 - 17	17 - 18	18 - 19	19 - 20	>20	Sum	
0,00	0,01	5,2280			0,0805	0,0906	0,0694	0,0962	0,1128	0,1443	0,1665	0,0768	0,0657	0,0213	0,0139	0,0028	0,0018				6,1705	
0,01	0,02				0,0416	0,1147	0,0657	0,0823	0,0509	0,0925	0,1073	0,1073	0,0592	0,0398	0,0203	0,0074	0,0018	0,0018			0,7927	
0,02	0,03				0,0102	0,0305	0,0573	0,0277	0,0490	0,0601	0,0629	0,0777	0,0490	0,0194	0,0120	0,0055	0,0018				0,4634	
0,03	0,04					0,0055	0,0620	0,0324	0,0222	0,0250	0,0314	0,0305	0,0296	0,0213	0,0129	0,0037	0,0018	0,0009			0,2793	
0,04	0,05							0,0296	0,0694	0,0287	0,0129	0,0055	0,0185	0,0176	0,0203	0,0092	0,0018				0,2137	
0,05	0,06							0,0092	0,0370	0,0333	0,0083	0,0065	0,0102	0,0046	0,0065	0,0055	0,0018				0,1230	
0,06	0,07							0,0046	0,0213	0,0314	0,0166	0,0037	0,0028		0,0009	0,0009	0,0055	0,0009			0,0888	
0,07	0,08								0,0046	0,0194	0,0157	0,0055	0,0009	0,0009							0,0472	
0,08	0,09									0,0009	0,0139										0,0148	
0,09	0,10									0,0028	0,0046										0,0074	
0,10	0,11									0,0018	0,0018	0,0009									0,0046	
0,11	0,12										0,0009	0,0009									0,0018	
0,12	0,13											0,0018									0,0018	
0,13	0,14											0,0028									0,0028	
0,14	0,15											0,0009									0,0009	
0,15	0,16											0,0009									0,0009	
0,16	0,17																				0,0000	
0,17	0,18																				0,0000	
0,18	0,19																				0,0000	
0,19	0,20																				0,0000	
0,20	0,21																				0,0000	
0,21	0,22																				0,0000	
0,22	0,23																				0,0000	
Sum		5,2280	0,0000	0,0000	0,0000	0,1323	0,2414	0,2978	0,3709	0,3515	0,3959	0,3922	0,3330	0,2266	0,1295	0,0749	0,0287	0,0083	0,0028	0,0000	0,0000	8,2138

Swell, Scatter diagram, July																						
Hm0	Tp																					
	<2	2 - 3	3 - 4	4 - 5	5 - 6	6 - 7	7 - 8	8 - 9	9 - 10	10 - 11	11 - 12	12 - 13	13 - 14	14 - 15	15 - 16	16 - 17	17 - 18	18 - 19	19 - 20	>20	Sum	
0,00	0,01	5,3556			0,5087	0,3062	0,1933	0,2553	0,2211	0,1017	0,0610	0,0213	0,0092	0,0009	0,0009						7,0363	
0,01	0,02				0,1156	0,2655	0,1276	0,0953	0,1230	0,1221	0,0536	0,0250	0,0102	0,0046	0,0055						0,9481	
0,02	0,03				0,0009	0,0213	0,0731	0,0314	0,0185	0,0324	0,0370	0,0203	0,0092	0,0028	0,0028						0,2497	
0,03	0,04					0,0009	0,0536	0,0222	0,0018	0,0018	0,0092	0,0139	0,0074	0,0018							0,1128	
0,04	0,05						0,0194	0,0527	0,0139		0,0009	0,0028	0,0009	0,0028	0,0028		0,0009				0,0971	
0,05	0,06							0,0148	0,0092		0,0018										0,0259	
0,06	0,07							0,0055	0,0055	0,0018											0,0129	
0,07	0,08								0,0028	0,0009											0,0037	
0,08	0,09									0,0009											0,0009	
0,09	0,10																				0,0000	
0,10	0,11																				0,0000	
0,11	0,12																				0,0000	
0,12	0,13																				0,0000	
0,13	0,14																				0,0000	
0,14	0,15																				0,0000	
0,15	0,16																				0,0000	
0,16	0,17																				0,0000	
0,17	0,18																				0,0000	
0,18	0,19																				0,0000	
0,19	0,20																				0,0000	
0,20	0,21																				0,0000	
0,21	0,22																				0,0000	
0,22	0,23																				0,0000	
Sum		5,3556	0,0000	0,0000	0,0000	0,6253	0,5938	0,4671	0,4773	0,3959	0,2636	0,1619	0,0832	0,0370	0,0129	0,0120	0,0009	0,0009	0,0000	0,0000	0,0000	8,4876

Swell, Scatter diagram, August																						
Hm0	Tp																					
	<2	2 - 3	3 - 4	4 - 5	5 - 6	6 - 7	7 - 8	8 - 9	9 - 10	10 - 11	11 - 12	12 - 13	13 - 14	14 - 15	15 - 16	16 - 17	17 - 18	18 - 19	19 - 20	>20	Sum	
0,00	0,01	5,2169			0,3635	0,2904	0,1693	0,2627	0,2645	0,1730	0,0684	0,0250	0,0166	0,0046	0,0028						6,8578	
0,01	0,02				0,0601	0,2285	0,1230	0,0934	0,1221	0,1360	0,0592	0,0370	0,0111	0,0046	0,0018	0,0018					0,8787	
0,02	0,03				0,0083	0,0296	0,0990	0,0305	0,0111	0,0388	0,0398	0,0398	0,0065	0,0028	0,0028						0,3089	
0,03	0,04						0,0990	0,0592	0,0028	0,0028	0,0111	0,0166	0,0065	0,0028	0,0009						0,2016	
0,04	0,05							0,0287	0,0647	0,0250	0,0018	0,0028	0,0018	0,0009	0,0028						0,1286	
0,05	0,06							0,0009	0,0231	0,0222	0,0037	0,0018		0,0009	0,0009						0,0536	
0,06	0,07								0,0065	0,0139	0,0074	0,0009	0,0009								0,0296	
0,07	0,08									0,0046	0,0046										0,0092	
0,08	0,09									0,0028	0,0046	0,0028									0,0102	
0,09	0,10										0,0009	0,0046									0,0055	
0,10	0,11								0,0009	0,0018		0,0009									0,0037	
0,11	0,12																				0,0000	
0,12	0,13																				0,0000	
0,13	0,14																				0,0000	
0,14	0,15																				0,0000	
0,15	0,16																				0,0000	
0,16	0,17																				0,0000	
0,17	0,18																				0,0000	
0,18	0,19																				0,0000	
0,19	0,20																				0,0000	
0,20	0,21																				0,0000	
0,21	0,22																				0,0000	
0,22	0,23																				0,0000	
Sum		5,2169	0,0000	0,0000	0,0000	0,4320	0,5485	0,5198	0,5402	0,4699	0,3755	0,1896	0,1239	0,0416	0,0157	0,0120	0,0018	0,0000	0,0000	0,0000	0,0000	8,4876

Swell, Scatter diagram, September																						
Hm0	Tp																					
	<2	2 - 3	3 - 4	4 - 5	5 - 6	6 - 7	7 - 8	8 - 9	9 - 10	10 - 11	11 - 12	12 - 13	13 - 14	14 - 15	15 - 16	16 - 17	17 - 18	18 - 19	19 - 20	>20	Sum	
0,00	0,01	4,7738			0,1101	0,1239	0,1147	0,1646	0,1406	0,1128	0,0897	0,0435	0,0240	0,0111	0,0065	0,0065	0,0028	0,0009			5,7256	
0,01	0,02				0,0629	0,1397	0,0814	0,1424	0,1239	0,0971	0,0897	0,0814	0,0453	0,0157	0,0046	0,0046	0,0037	0,0009			0,8935	
0,02	0,03				0,0083	0,0444	0,0823	0,0425	0,0620	0,0657	0,0601	0,0731	0,0305	0,0203	0,0139	0,0028	0,0009				0,5069	
0,03	0,04					0,0046	0,1064	0,0629	0,0129	0,0166	0,0314	0,0240	0,0120	0,0018	0,0046	0,0009	0,0018				0,2803	
0,04	0,05						0,0518	0,0860	0,0407	0,0111	0,0166	0,0120	0,0111	0,0065	0,0046						0,2405	
0,05	0,06						0,0139	0,0999	0,0851	0,0120	0,0046	0,0129	0,0009	0,0046	0,0028						0,2368	
0,06	0,07						0,0037	0,0416	0,0768	0,0222		0,0037	0,0018	0,0009	0,0028						0,1535	
0,07	0,08							0,0065	0,0268	0,0268	0,0018		0,0037	0,0028	0,0028						0,0712	
0,08	0,09							0,0009	0,0111	0,0166	0,0065					0,0009					0,0361	
0,09	0,10								0,0092	0,0157	0,0055										0,0305	
0,10	0,11								0,0018	0,0065	0,0065	0,0018									0,0166	
0,11	0,12									0,0028	0,0009	0,0009									0,0046	
0,12	0,13									0,0009	0,0009	0,0018									0,0037	
0,13	0,14									0,0018		0,0018	0,0009	0,0009							0,0055	
0,14	0,15										0,0018		0,0018								0,0037	
0,15	0,16										0,0028	0,0009									0,0037	
0,16	0,17											0,0009									0,0009	
0,17	0,18																				0,0000	
0,18	0,19																				0,0000	
0,19	0,20																				0,0000	
0,20	0,21																				0,0000	
0,21	0,22																				0,0000	
0,22	0,23																				0,0000	
Sum		4,7738	0,0000	0,0000	0,0000	0,1813	0,3126	0,4542	0,6475	0,5911	0,4088	0,3191	0,2590	0,1323	0,0647	0,0425	0,0157	0,0092	0,0018	0,0000	0,0000	8,2138

Swell, Scatter diagram, October																						
Hm0	Tp																					
	<2	2 - 3	3 - 4	4 - 5	5 - 6	6 - 7	7 - 8	8 - 9	9 - 10	10 - 11	11 - 12	12 - 13	13 - 14	14 - 15	15 - 16	16 - 17	17 - 18	18 - 19	19 - 20	>20	Sum	
0,00	0,01	5,2289			0,0388	0,0610	0,0934	0,1101	0,1323	0,1369	0,0860	0,0610	0,0240	0,0092	0,0074	0,0037	0,0018				5,9948	
0,01	0,02				0,0231	0,0888	0,0749	0,1156	0,0832	0,0592	0,0573	0,0435	0,0333	0,0259	0,0166	0,0065	0,0037	0,0009			0,6327	
0,02	0,03				0,0102	0,0536	0,0842	0,0527	0,0731	0,0740	0,0657	0,0546	0,0277	0,0166	0,0148	0,0046	0,0046	0,0009			0,5374	
0,03	0,04					0,0102	0,0620	0,0555	0,0203	0,0296	0,0259	0,0370	0,0268	0,0166	0,0046	0,0018	0,0009	0,0009			0,2923	
0,04	0,05						0,0416	0,1128	0,0453	0,0037	0,0176	0,0194	0,0222	0,0166	0,0102	0,0028	0,0037	0,0009			0,2969	
0,05	0,06						0,0240	0,0842	0,0647	0,0120	0,0065	0,0046	0,0055	0,0028	0,0037	0,0111					0,2192	
0,06	0,07						0,0065	0,0444	0,0795	0,0231	0,0018	0,0046	0,0009	0,0018	0,0009	0,0009		0,0028	0,0009		0,1683	
0,07	0,08							0,0139	0,0472	0,0361	0,0037		0,0009				0,0009	0,0009	0,0009		0,1045	
0,08	0,09							0,0037	0,0259	0,0407	0,0065			0,0009				0,0009			0,0786	
0,09	0,10								0,0129	0,0407	0,0166	0,0009			0,0009	0,0009					0,0731	
0,10	0,11								0,0009	0,0176	0,0092	0,0009									0,0287	
0,11	0,12								0,0009	0,0083	0,0102	0,0009									0,0203	
0,12	0,13									0,0009	0,0055	0,0018									0,0083	
0,13	0,14										0,0009	0,0083									0,0092	
0,14	0,15										0,0009	0,0037	0,0037								0,0083	
0,15	0,16										0,0009	0,0092	0,0009	0,0009							0,0120	
0,16	0,17																				0,0000	
0,17	0,18											0,0009									0,0009	
0,18	0,19											0,0009		0,0009							0,0018	
0,19	0,20																				0,0000	
0,20	0,21																				0,0000	
0,21	0,22																				0,0000	
0,22	0,23																				0,0000	
Sum		5,2289	0,0000	0,0000	0,0000	0,0721	0,2137	0,3866	0,5929	0,5864	0,4828	0,3154	0,2525	0,1461	0,0925	0,0592	0,0324	0,0185	0,0065	0,0009	0,0000	8,4876

Swell, Scatter diagram, November																						
Hm0	Tp																					
	<2	2 - 3	3 - 4	4 - 5	5 - 6	6 - 7	7 - 8	8 - 9	9 - 10	10 - 11	11 - 12	12 - 13	13 - 14	14 - 15	15 - 16	16 - 17	17 - 18	18 - 19	19 - 20	>20	Sum	
0,00	0,01	4,9791			0,0222	0,0499	0,0703	0,0564	0,0731	0,0916	0,0888	0,0379	0,0277	0,0092	0,0074	0,0009					5,5147	
0,01	0,02				0,0324	0,0536	0,0629	0,0823	0,1073	0,0749	0,0518	0,0564	0,0555	0,0250	0,0139	0,0065	0,0037	0,0009			0,6271	
0,02	0,03				0,0120	0,0416	0,0481	0,0453	0,0629	0,0666	0,0518	0,0749	0,0610	0,0444	0,0259	0,0018					0,5374	
0,03	0,04				0,0009	0,0037	0,0536	0,0416	0,0342	0,0564	0,0490	0,0351	0,0324	0,0213	0,0102	0,0074	0,0037				0,3496	
0,04	0,05						0,0453	0,0860	0,0351	0,0092	0,0287	0,0333	0,0139	0,0148	0,0083	0,0009	0,0009	0,0018			0,2784	
0,05	0,06						0,0287	0,0777	0,0518	0,0148	0,0083	0,0194	0,0129	0,0083	0,0055	0,0074	0,0028				0,2377	
0,06	0,07						0,0102	0,0453	0,0749	0,0435	0,0083	0,0074	0,0028	0,0055	0,0046	0,0092	0,0009	0,0009			0,2137	
0,07	0,08						0,0037	0,0111	0,0425	0,0361	0,0065	0,0037	0,0028		0,0009	0,0046	0,0009	0,0009			0,1138	
0,08	0,09						0,0009	0,0046	0,0398	0,0555	0,0213	0,0037	0,0009		0,0018						0,1295	
0,09	0,10							0,0009	0,0157	0,0342	0,0166	0,0009									0,0694	
0,10	0,11								0,0055	0,0203	0,0185	0,0028	0,0009								0,0481	
0,11	0,12									0,0139	0,0176	0,0028						0,0009			0,0351	
0,12	0,13									0,0046	0,0037	0,0083	0,0009								0,0176	
0,13	0,14									0,0018	0,0046	0,0037	0,0018				0,0009				0,0129	
0,14	0,15										0,0009	0,0055	0,0009				0,0009				0,0083	
0,15	0,16										0,0028	0,0065									0,0092	
0,16	0,17										0,0018	0,0037	0,0009								0,0065	
0,17	0,18											0,0028									0,0028	
0,18	0,19											0,0018									0,0018	
0,19	0,20																				0,0000	
0,20	0,21																				0,0000	
0,21	0,22																				0,0000	
0,22	0,23																				0,0000	
Sum		4,9791	0,0000	0,0000	0,0000	0,0675	0,1489	0,3237	0,4514	0,5430	0,5235	0,3811	0,3108	0,2155	0,1286	0,0768	0,0407	0,0148	0,0083	0,0000	0,0000	8,2138
Swell, Scatter diagram, December																						
Hm0	Tp																					
	<2	2 - 3	3 - 4	4 - 5	5 - 6	6 - 7	7 - 8	8 - 9	9 - 10	10 - 11	11 - 12	12 - 13	13 - 14	14 - 15	15 - 16	16 - 17	17 - 18	18 - 19	19 - 20	>20	Sum	
0,00	0,01	4,8450			0,0370	0,0481	0,0453	0,0583	0,0435	0,0768	0,0897	0,0694	0,0333	0,0139	0,0083	0,0074	0,0009	0,0018			5,3787	
0,01	0,02				0,0176	0,0324	0,0564	0,0888	0,0906	0,0647	0,0555	0,0860	0,0721	0,0324	0,0231	0,0074	0,0018	0,0028			0,6318	
0,02	0,03				0,0120	0,0250	0,0518	0,0435	0,0795	0,0749	0,0638	0,0435	0,0407	0,0425	0,0305	0,0111	0,0028	0,0018			0,5235	
0,03	0,04					0,0074	0,0601	0,0481	0,0324	0,0518	0,0546	0,0379	0,0296	0,0268	0,0259	0,0120	0,0046				0,3913	
0,04	0,05					0,0009	0,0629	0,0980	0,0462	0,0148	0,0268	0,0324	0,0231	0,0148	0,0166	0,0203	0,0046	0,0046			0,3663	
0,05	0,06						0,0222	0,0906	0,0805	0,0166	0,0148	0,0139	0,0092	0,0083	0,0037	0,0083	0,0083	0,0083	0,0009		0,2858	
0,06	0,07						0,0055	0,0684	0,1091	0,0351	0,0102	0,0083	0,0037	0,0009	0,0055	0,0102	0,0046	0,0037			0,2655	
0,07	0,08						0,0055	0,0240	0,0731	0,0481	0,0055	0,0037	0,0037	0,0046	0,0028	0,0018	0,0028	0,0046			0,1804	
0,08	0,09							0,0037	0,0490	0,0472	0,0213	0,0009		0,0009	0,0037		0,0009	0,0018			0,1295	
0,09	0,10							0,0009	0,0102	0,0370	0,0250	0,0046		0,0018							0,0795	
0,10	0,11								0,0065	0,0324	0,0222	0,0037	0,0009								0,0657	
0,11	0,12								0,0018	0,0194	0,0342	0,0055		0,0009	0,0009						0,0629	
0,12	0,13									0,0157	0,0277	0,0065	0,0018								0,0518	
0,13	0,14									0,0028	0,0111	0,0083	0,0018					0,0009			0,0250	
0,14	0,15										0,0046	0,0074	0,0028								0,0148	
0,15	0,16									0,0009	0,0046	0,0083		0,0009	0,0009						0,0157	
0,16	0,17										0,0018	0,0055	0,0018								0,0092	
0,17	0,18											0,0018	0,0009								0,0028	
0,18	0,19													0,0009							0,0028	
0,19	0,20													0,0009							0,0009	
0,20	0,21													0,0028							0,0028	
0,21	0,22																				0,0000	
0,22	0,23																				0,0000	
Sum		4,8450	0,0000	0,0000	0,0000	0,0666	0,1138	0,3099	0,5245	0,6225	0,5383	0,4736	0,3496	0,2257	0,1535	0,1221	0,0786	0,0314	0,0305	0,0009	0,0000	8,4866

Appendix C

Directional distribution of wind

Probability [%] of wind directions within wave sectors, All sea states												
Wind direction	Wave direction											
	345 - 15	15 - 45	45 - 75	75 - 105	105 - 135	135 - 165	165 - 195	195 - 225	225 - 255	255 - 285	285 - 315	315 - 345
0 - 10	0,12948741	0,04241829	0,04092993	0,02976722	0,01339525	0,01562779	0,04167411	0,03944157	0,01711615	0,01711615	0,14958028	0,30585819
10 - 20	0,09079002	0,06027862	0,03944157	0,03348812	0,01488361	0,01786033	0,04613919	0,03572066	0,01860451	0,02381378	0,08632494	0,16967316
20 - 30	0,08185986	0,07218551	0,06697625	0,04539501	0,01934869	0,02232542	0,04688337	0,05209264	0,01860451	0,01934869	0,05581354	0,12204560
30 - 40	0,08558076	0,08483658	0,10567363	0,06995297	0,02381378	0,02902304	0,05358100	0,03720903	0,00967435	0,02753468	0,05358100	0,08334822
40 - 50	0,08037149	0,06176698	0,15181282	0,13767339	0,03348812	0,03572066	0,06325534	0,03274394	0,02009287	0,02232542	0,04167411	0,06325534
50 - 60	0,06697625	0,06176698	0,22623087	0,28130023	0,05134846	0,05358100	0,07739477	0,06623207	0,01860451	0,02158123	0,04837173	0,05804608
60 - 70	0,08632494	0,09525511	0,36688099	0,62511163	0,11758052	0,09599929	0,11162708	0,09153420	0,03944157	0,04018575	0,04837173	0,05879026
70 - 80	0,12204560	0,19125439	0,43460142	1,34919926	0,25004465	0,17860332	0,21209144	0,14809192	0,05655772	0,04837173	0,07367387	0,09525511
80 - 90	0,18678931	0,31776508	0,49562422	2,41784247	0,46883372	0,30957909	0,30734655	0,27013752	0,10939453	0,08334822	0,10939453	0,12874323
90 - 100	0,27981187	0,36613681	0,43088051	2,60686432	0,66901828	0,40036911	0,40706674	0,34157885	0,13097577	0,11311544	0,12948741	0,18678931
100 - 110	0,20837054	0,23813776	0,31702090	2,42081919	0,71143657	0,36316009	0,32967197	0,25823064	0,08632494	0,07144133	0,08855748	0,13618503
110 - 120	0,13692921	0,13023159	0,16818479	1,43329166	0,72483182	0,33562541	0,28055605	0,16669643	0,05730190	0,03720903	0,07888313	0,08260404
120 - 130	0,09972019	0,09525511	0,08706912	0,81487766	0,72855272	0,42195035	0,20539382	0,13841757	0,05358100	0,03720903	0,05209264	0,07144133
130 - 140	0,08706912	0,07590641	0,05060427	0,47478716	0,85878431	0,64818122	0,26269572	0,19274275	0,04539501	0,03720903	0,04167411	0,04613919
140 - 150	0,09376674	0,07144133	0,05506936	0,36985771	0,97934155	1,45784962	0,46436864	0,30213729	0,04241829	0,03572066	0,05432518	0,05804608
150 - 160	0,07962731	0,07665059	0,05804608	0,27832351	0,76873847	2,89783890	1,00538787	0,50306602	0,06623207	0,04092993	0,03944157	0,06474370
160 - 170	0,06548788	0,03720903	0,03051140	0,12427814	0,28725368	1,5998809	1,19143299	0,59385605	0,04911591	0,02679050	0,03199976	0,04465083
170 - 180	0,05283682	0,03348812	0,02232542	0,04688337	0,11013872	0,49711258	0,85134250	0,76278502	0,04762755	0,02753468	0,03795321	0,02976722
180 - 190	0,03720903	0,03199976	0,01860451	0,04390665	0,06251116	0,20241710	0,55441448	1,35961779	0,07888313	0,04613919	0,04092993	0,03944157
190 - 200	0,05804608	0,05358100	0,03348812	0,04092993	0,07069715	0,18604513	0,47925225	2,74677026	0,20241710	0,07292969	0,04837173	0,03795321
200 - 210	0,06474370	0,07292969	0,03944157	0,06251116	0,07813895	0,17413824	0,39813657	3,40164910	0,44129904	0,14139430	0,06697625	0,05953444
210 - 220	0,05506936	0,05134846	0,02753468	0,05209264	0,05953444	0,09004584	0,24632375	1,52705840	0,44501994	0,16892898	0,07590641	0,05506936
220 - 230	0,06548788	0,04018575	0,02604632	0,03348812	0,02902304	0,05655772	0,11460380	0,70845984	0,59832113	0,19051021	0,09079002	0,05283682
230 - 240	0,05953444	0,04613919	0,02530214	0,01860451	0,02009287	0,03869739	0,09302256	0,43162469	0,60055367	0,28278859	0,11534798	0,05506936
240 - 250	0,06920879	0,03944157	0,02083705	0,01413943	0,02232542	0,04241829	0,07441805	0,27311425	0,50232184	0,48446151	0,14362684	0,06697625
250 - 260	0,08260404	0,06772043	0,02604632	0,02381378	0,02604632	0,04018575	0,09302256	0,25971900	0,33413705	0,70622730	0,23962612	0,07665059
260 - 270	0,08409240	0,06102280	0,02753468	0,03348812	0,02455796	0,04688337	0,09227838	0,18976603	0,21878907	0,72780854	0,38697386	0,08930166
270 - 280	0,11534798	0,07292969	0,04092993	0,03051140	0,02306960	0,05506936	0,10790617	0,14437102	0,17190570	0,56111210	0,78883134	0,11460380
280 - 290	0,15330118	0,09599929	0,04018575	0,03423230	0,03125558	0,07441805	0,09972019	0,14511520	0,14883610	0,43608978	1,16017741	0,17339406
290 - 300	0,15181282	0,10418527	0,04465083	0,03795321	0,03348812	0,06995297	0,11162708	0,14809192	0,11683634	0,29023040	0,95478359	0,15330118
300 - 310	0,15255700	0,08855748	0,04613919	0,04018575	0,03869739	0,05283682	0,12130142	0,12799905	0,08483658	0,18902185	1,22566530	0,19125439
310 - 320	0,12278978	0,06846461	0,04911591	0,03646484	0,03646484	0,05209264	0,08409240	0,09748765	0,08930166	0,15702209	2,56519021	0,28874204
320 - 330	0,09674347	0,04688337	0,04539501	0,03348812	0,02604632	0,02827886	0,08409240	0,08185986	0,08111568	0,11832470	3,52964815	0,41674108
330 - 340	0,09823183	0,04316247	0,03199976	0,03125558	0,01190689	0,03423230	0,04986009	0,06027862	0,03646484	0,07218551	2,06138001	0,63478597
340 - 350	0,12278978	0,04762755	0,03720903	0,02604632	0,02009287	0,02753468	0,05358100	0,04986009	0,03274394	0,03199976	0,83497053	0,85431922
350 - 360	0,16074299	0,05209264	0,02976722	0,02232542	0,01116271	0,02158123	0,04837173	0,03051140	0,02232542	0,02530214	0,31553254	0,71887837

Appendix D

Distribution of Tidal Amplitudes

A comparison between water level observed by the Kartverket's tidal stations in Bergen and water level measurements made in the Bjørnafjord [22] show a linear relationship between the water levels. In the future the analysis of tidal conditions in Bjørnafjord can therefore be performed by using data measured in Bergen and scaling it by a factor.

$$H_{Bfj} = 0.85H_{Bergen}$$

where,

H_{Bfj} = Tidal height measured at the Bjørnafjord

H_{Bergen} = Tidal height measured at Bergen

Factor = 0.85

Tidal water level has been measured in Bjørnafjord from January 2015 to April 2018. The following figure shows the distribution of the tidal amplitudes (difference between the high tide level and low tide level for a particular semidiurnal tidal cycle). [22]

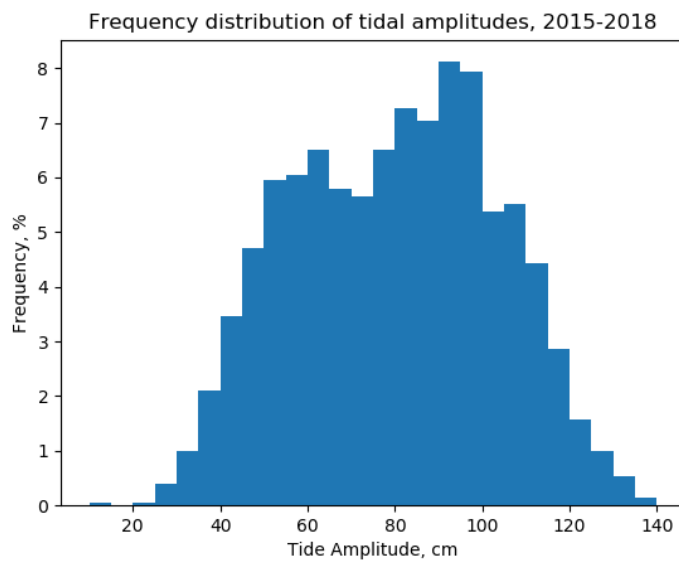


Figure 6 Distribution of tidal amplitudes.

Index	Bin (cm)	Frequency (%)	Frequency (N)	Index	Bin (cm)	Frequency (%)	Frequency (N)
1	10 to 15	0.045	1	14	75 to 80	6.502	145
2	15 to 20	0.000	0	15	80 to 85	7.265	162
3	20 to 25	0.045	1	16	85 to 90	7.040	157
4	25 to 30	0.404	9	17	90 to 95	8.117	181
5	30 to 35	0.987	22	18	95 to 100	7.937	177
6	35 to 40	2.108	47	19	100 to 105	5.381	120
7	40 to 45	3.453	77	20	105 to 110	5.516	123
8	45 to 50	4.709	105	21	110 to 115	4.439	99
9	50 to 55	5.964	133	22	115 to 120	2.870	64
10	55 to 60	6.054	135	23	120 to 125	1.570	35
11	60 to 65	6.502	145	24	125 to 130	0.987	22
12	65 to 70	5.785	129	25	130 to 135	0.538	12
13	70 to 75	5.650	126	26	135 to 140	0.135	3
Total							2230

The following figure shows the distribution of the surge component levels for the same measurement period (January 2015 to April 2018).

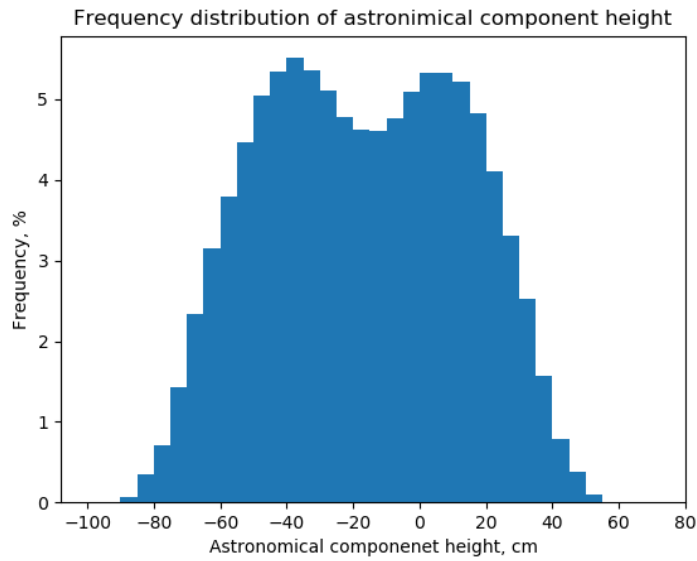


Figure 7 Distribution of water level due to the astronomical component.

Index	Bin (cm)	Frequency (%)	Frequency (N)	Index	Bin (cm)	Frequency (%)	Frequency (N)
1	-100 to -95	0.000	0	17	-20 to -15	4.621	6618
2	-95 to -90	0.000	0	18	-15 to -10	4.602	6591
3	-90 to -85	0.072	103	19	-10 to -5	4.772	6834
4	-85 to -80	0.342	490	20	-5 to 0	5.094	7295
5	-80 to -75	0.709	1015	21	0 to 5	5.327	7628
6	-75 to -70	1.421	2035	22	5 to 10	5.321	7620
7	-70 to -65	2.343	3356	23	10 to 15	5.225	7482
8	-65 to -60	3.152	4514	24	15 to 20	4.829	6916
9	-60 to -55	3.797	5438	25	20 to 25	4.109	5884
10	-55 to -50	4.470	6402	26	25 to 30	3.302	4729
11	-50 to -45	5.042	7220	27	30 to 35	2.519	3607
12	-45 to -40	5.338	7644	28	35 to 40	1.577	2258
13	-40 to -35	5.513	7895	29	40 to 45	0.779	1116
14	-35 to -30	5.363	7680	30	45 to 50	0.376	538
15	-30 to -25	5.115	7325	31	50 to 55	0.092	132
16	-25 to -20	4.777	6841	32	55 to 60	0.001	1
Total							143207

The following figure shows the distribution of the surge component levels for the same measurement period (January 2015 to April 2018).

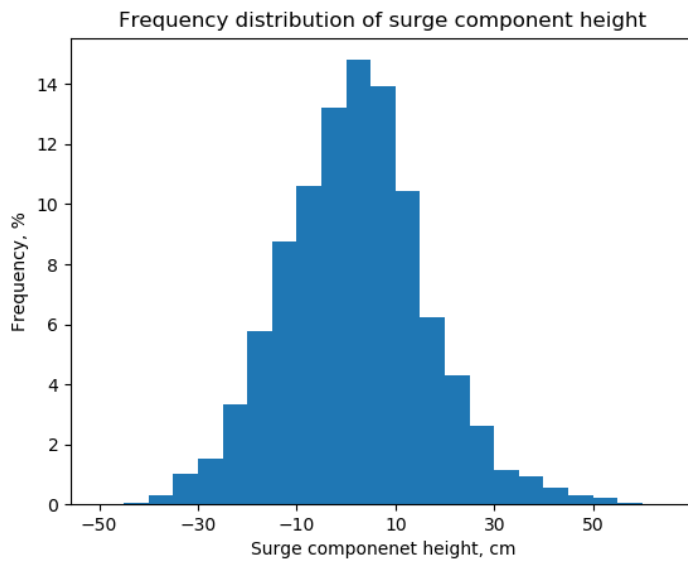


Figure 8 Distribution of water level due to the surge component.

Index	Bin (cm)	Frequency (%)	Frequency (N)	Index	Bin (cm)	Frequency (%)	Frequency (N)
1	-50 to -45	0.001	1	13	10 to 15	10.43	14930
2	-45 to -40	0.036	51	14	15 to 20	6.22	8905
3	-40 to -35	0.293	419	15	20 to 25	4.32	6180
4	-35 to -30	1.012	1449	16	25 to 30	2.60	3723
5	-30 to -25	1.531	2192	17	30 to 35	1.13	1623
6	-25 to -20	3.321	4756	18	35 to 40	0.92	1320
7	-20 to -15	5.771	8264	19	40 to 45	0.56	809
8	-15 to -10	8.767	12555	20	45 to 50	0.31	447
9	-10 to -5	10.594	15171	21	50 to 55	0.20	290
10	-5 to 0	13.196	18897	22	55 to 60	0.03	44
11	0 to 5	14.806	21203	23	60 to 65	0.01	14
12	5 to 10	13.929	19948	24	65 to 70	0.00	0
Total							143207